Gauge-invariant three-boson vertices and their Ward identities in the standard model

Joannis Papavassiliou and Kostas Philippides
Department of Physics, New York University, Andre and Bella Meyer Hall of Physics, 4 Washington Place, New York, New York 10003
(Received 13 March 1995)

In the context of the standard model we extend the S-matrix pinch technique for nonconserved currents to the case of three-boson vertices. We outline in detail how effective gauge-invariant three-boson vertices can be constructed, with all three incoming momenta *off shell*. Explicit closed expressions for the vertices γW^-W^+, ZW^-W^+, and χW^-W^+ are reported. The three-boson vertices so constructed satisfy naive QED-like Ward identities which relate them to the gauge-invariant gauge boson self-energies previously constructed by the same method. The derivation of the aforementioned Ward identities relies on the sole requirement of complete gauge invariance of the S-matrix element considered; in particular, no knowledge of the explicit closed form of the three-boson vertices involved is necessary. The validity of one of these Ward identities is demonstrated explicitly, through a detailed diagrammatic one-loop analysis, in the context of three different gauges.

PACS number(s): 11.15.Bt, 11.15.Ex, 12.15.Lk

I. INTRODUCTION

The pinch technique (PT) is an algorithm that allows the construction of modified gauge-independent (GI) off-shell n-point functions, through the order-by-order rearrangement of Feynman graphs contributing to a certain physical and therefore ostensibly GI amplitude, such as an S-matrix element or a Wilson loop [1]. The PT was originally introduced in an attempt to gain insight from perturbation theory on issues encountered in developing a consistent truncation scheme for the Schwinger-Dyson (SD) equations governing the nonperturbative QCD dynamics [2]. Specifically, one wishes to construct a SD series which is manifestly GI already in its one-dressed loop truncated version. This is a nontrivial task, since the mechanism of gauge cancellations is very subtle and involves in general a delicate conspiracy of terms coming from all orders.

The systematic derivation of such a SD series for QCD has been the focal point of extensive research [3,4]. Of particular interest in this context is the study of the three-gluon vertex $\hat{\Gamma}_3$ [5] and the four-gluon vertex $\hat{\Gamma}_4$ [6]. In particular, as explained first in [4] and later in [6], one attempts to construct an effective potential Ω [7] for quarkless QCD, which, in ghost-free gauges, is a functional of only three basic quantities: the gluon self-energy ($\hat{d}$), the three gluon vertex ($\hat{\Gamma}_3$), and the four gluon vertex ($\hat{\Gamma}_4$), e.g., $\Omega(\hat{d},\hat{\Gamma}_3,\hat{\Gamma}_4)$. One then requires that Ω be manifestly gauge independent for *off-shell* $\hat{d}$, $\hat{\Gamma}_3$, and $\hat{\Gamma}_4$, e.g., when they do not necessarily satisfy their respective SD equations. This requirement can be enforced if $\hat{d}$, $\hat{\Gamma}_3$, and $\hat{\Gamma}_4$ are individually gauge independent and, at the same time, the renormalized self energy $\hat{\Pi}_{\mu\nu}$ is transverse, e.g.,

$$q^\mu \hat{\Pi}_{\mu\nu} = 0, \tag{1.1}$$

order by order in the dressed loop expansion [8]. The one-loop dressed expression for $\hat{\Pi}_{\mu\nu}$ is schematically shown in Fig. 1; we see that already at this level the fully dressed vertices $\hat{\Gamma}_3$ and $\hat{\Gamma}_4$ make their appearance. It turns out that Eq. (1.1) can be satisfied as long as $\hat{d}$, $\hat{\Gamma}_3$, and $\hat{\Gamma}_4$ satisfy the Ward identities (WI's)

$$q_1^\mu \hat{\Gamma}_{\mu\nu\alpha}(q_1,q_2,q_3) = T_{\nu\alpha}(q_2)\hat{d}^{-1}(q_2) - T_{\nu\alpha}(q_3)\hat{d}^{-1}(q_3), \tag{1.2}$$

$$q_1^\mu \hat{\Gamma}^{abcd}_{\mu\nu\alpha\beta} = f_{abp}\hat{\Gamma}^{cdp}_{\nu\alpha\beta}(q_1+q_2,q_3,q_4) + \text{c.p.}, \tag{1.3}$$

where

$$\hat{d}^{-1}(q) = q^2 - \hat{\Pi}(q)\ . \tag{1.4}$$

$T_{\mu\nu}(q) = g_{\mu\nu} - q_\mu q_\nu/q^2$ is the usual transverse projection operator, f^{abc} the structure constants of the gauge group, and the abbreviation c.p. in the right-hand side (RHS) of Eq. (1.3) stands for "cyclic permutations" [9].

Although this program has been layed out conceptually, its practical implementation is as yet incomplete. One thing is certain, however: If Green's functions with the properties described above can arise out of a self-

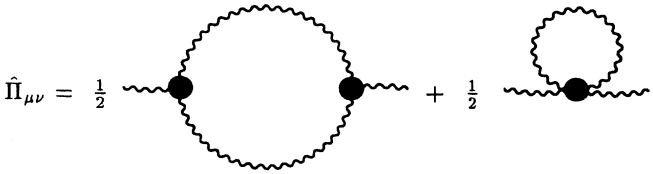

FIG. 1. One-loop-dressed Feynman graphs for the renormalized $\hat{\Pi}_{\mu\nu}$ (in a ghost-free gauge) necessary to implement the gauge invariance of the effective potential. All vertices and propagators are fully dressed.

consistent treatment of QCD, one should be able to construct Green's functions with the same properties at the level of ordinary perturbation theory after appropriate rearrangement of Feynman graphs. The PT accomplishes this task by providing the systematic algorithm needed to recover the desired Green's functions order by order in perturbation theory. So GI three- and four-gluon vertices have already been constructed via the PT at one loop, and they satisfy the Ward identities of Eqs. (1.2) and (1.3) [10].

A program similar to that outlined above for QCD has also been proposed for the case of non-Abelian gauge theories with either elementary Higgs particles or with dynamical symmetry breaking [11]. In an attempt to study the general structure of the GI Green's functions involved, the PT was extended to the case of theories with tree-level symmetry breaking. The technical modifications necessary to accomplish such a task have been presented in [12] in the context of an SU(2) toy model. The upshot of that analysis was that the PT, when properly applied, gives rise to GI two- and three-point functions, which satisfy the same WI as in the symmetric (unbroken) case, provided one includes appropriate longitudinal Goldstone boson Green's functions. So, for example, Eq. (1.1) becomes

$$q^\mu \hat{\Pi}_{\mu\nu} + M\hat{\Pi}_\nu = 0, \tag{1.5}$$

where $\hat{\Pi}_\nu$ is the GI one-loop mixed self-energy between the (massive) gauge boson and the corresponding Goldstone boson. Clearly, Eq. (1.1) may be enforced if we redefine the gauge boson self-energy to be $\hat{\Pi}^{\rm tr}_{\mu\nu} = \hat{\Pi}_{\mu\nu} + \frac{Mq_\mu}{q^2}\hat{\Pi}_\nu$ with similar redefinitions for other n-point functions. Subsequently, the PT was extended to the full standard model (SM) [13], and several interesting applications were proposed [14–17].

Even though formal considerations similar to those of the QCD case would provide sufficient grounds for a detailed study of GI three- and four-gauge-boson vertices in the context of the SM, such a study was precipitated by phenomenological issues. In particular, the possibility of directly probing non-Abelian vertices in the upcoming experiments at the CERN e^+e^- collider LEP 2, through the process $e^+e^- \to W^+W^-$, has led to extensive studies of anomalous gauge boson couplings, induced either by extensions of the SM or by one-loop corrections within the SM [18–20]. In computing the latter, issues of gauge invariance become very important. So form factors of the W boson, such as the magnetic dipole and electric quadrupole moments, turn out to be gauge dependent when extracted from the conventional off-shell γWW and ZWW vertices calculated in the context of the R_ξ gauges [22]. In addition, these quantities are infrared divergent and violate perturbative unitarity. All the above pathologies can be bypassed, as long as one instead extracts them from GI off-shell γWW and ZWW vertices constructed via the PT [23].

Given the relevance of GI three-boson vertices (TBV's) both from the theoretical and the phenomenological point of view, we present in this paper the general methodology for their construction for the electroweak sector of the SM. We focus on the vertices involving one neutral and two charged incoming particles, with all three incoming momenta off shell. In order to construct such vertices, we consider a matrix element for six-fermion elastic scattering of the form $e^-e^-\nu \to e^-e^-\nu$, where the external electrons e are considered to be massive. This assumption is important, since, in addition to the GI vertices with three incoming gauge bosons (γW^+W^- and ZW^+W^-), it enables the construction of GI three-boson vertices where at least one of the incoming bosons is a scalar particle (unphysical would-be Goldstone bosons and physical Higgs boson). As we will see in what follows, the latter play a crucial role in the Ward identities, enforcing the gauge invariance of the S matrix. In particular, in this paper we focus on the following issues.

(a) We discuss the technical difficulties involved in the application of the PT when the necessary assumption is made that $m_e \neq 0$.

(b) We present the most general algorithm for constructing GI vertices involving one neutral and two charged bosons.

(c) We explain how the requirement of the gauge invariance of the S matrix gives rise to a set of WI's, relating several of the GI vertices to each other. The derivation is general and does not require knowledge of the explicit closed form of the quantities involved. Most noticeably, the WI

$$q^\mu \hat{\Gamma}^{ZW^-W^+}_{\mu\alpha\beta}(q,p_1,p_2) + iM_Z\hat{\Gamma}^{\chi W^-W^+}_{\alpha\beta}(q,p_1,p_2) = gc\left[\hat{\Pi}^W_{\alpha\beta}(p_1) - \hat{\Pi}^W_{\alpha\beta}(p_2)\right] \tag{1.6}$$

relates the GI vertices $\hat{\Gamma}^{ZW^-W^+}_{\mu\alpha\beta}$ and $\hat{\Gamma}^{\chi W^-W^+}_{\alpha\beta}$ to the GI W self-energy $\hat{\Pi}^W_{\alpha\beta}$. To the best of our knowledge, the WI we present here has not been derived before within the PT or any other framework.

There is one additional reason why the study of the GI vertices and WI's via the PT is interesting. As was recently realized, there is a close connection between the PT and the background field method (BFM) [24]. In particular, it was shown that in all cases considered so far the PT Green's functions may be obtained directly if one computes the conventional Green's functions in the context of the BFM using the special value $\xi_Q = 1$ of the gauge-fixing parameter used to gauge fix the quantum field [25,26]. Since, however, no formal connection between the two methods has yet been established, additional cases may have to be considered, at least for those Green's functions which are of particular physical relevance. The method for constructing vertices referred to above provides the framework for such a detailed investigation.

It is important to emphasize that the closed form of the GI TBV's obtained by the application of the S-matrix PT does *not* depend on the particular process employed. So instead of the process $ee\nu \to ee\nu$, one could equally well extract the GI TBV's from a process of the form $bbt \to bbt$, where t and b are the top and bottom quarks, respectively, or even a process involving gauge bosons

as external on-shell particles, such as $WW\gamma \to WW\gamma$. The fact that the PT gives rise to *process-independent* results had been conjectured before [12] and has been recently proved [28] via detailed calculations. Moreover, the PT algorithm gives rise to *exactly* the same answers, regardless of the gauge-fixing procedure chosen. This has been shown by explicit calculations for a wide variety of gauge-fixing choices, such as the R_ξ gauges, the light-cone gauge [2], the unitary gauge [29], and the background field gauges [25].

The paper is organized as follows: In Sec. I we briefly review some of the features of the PT, which are relevant to our purposes. In particular, we present a detailed analysis of the modifications necessary for the application of the PT in the context of the SM with nonconserved external currents. In Sec. II the method for constructing the GI vertices is described in detail. In Sec. III we apply the formalism developed in the previous section to a concrete example, and we perform an explicit one-loop calculation. In Sec. IV we outline the general method for obtaining WI's within the PT framework, and we derive a set of WI's for the newly constructed TBV's. In Sec. V we explicitly prove the first of the Ward identities derived in the previous section, to one-loop order, in the context of three different gauges. Finally, in Sec. VI we present our conclusions.

II. PINCH TECHNIQUE FOR NONCONSERVED CURRENTS

The simplest example that demonstrates how the PT works is the gluon two-point function (propagator). Consider the S-matrix element T for the $2 \to 2$ process of the elastic scattering of two fermions of masses m_1 and m_2:

$$q_1(p_1) + q_2(p_2) \to q_1(\hat{p}_1) + q_2(\hat{p}_2). \tag{2.1}$$

To any order in perturbation theory, T is independent of the gauge-fixing parameter one has to use to define the free gluon propagator. For example, in the covariant R_ξ gauges the gluon propagator is given by

$$\Delta_{\mu\nu}(q) = \frac{1}{q^2}\left[g_{\mu\nu} - (1-\xi)\frac{q_\mu q_\nu}{q^2}\right]. \tag{2.2}$$

On the other hand, as an explicit calculation shows, the conventionally defined proper self-energy depends on the gauge-fixing parameter, in this case ξ. At the one-loop level the gauge dependence of the self-energy graphs is canceled by contributions from other graphs, vertex, or box, which, at first glance, do not seem to be propagatorlike. That this cancellation must occur and can be employed to define a GI self-energy is evident from the decomposition:

$$\begin{aligned} T(s,t,m_1,m_2) = {} & T_1(t,\xi) + T_2(t,m_1,m_2,\xi) \\ & + T_3(s,t,m_1,m_2,\xi), \end{aligned} \tag{2.3}$$

where the function $T_1(t)$ depends only on the Mandelstam variable $t = -(\hat{p}_1 - p_1)^2 = -q^2$, and not on $s = (p_1 + p_2)^2$ or on the external masses. Typically, self-energy, vertex, and box diagrams contribute to T_1, T_2, and T_3, respectively. Moreover, such contributions are ξ dependent. However, as the sum $T(s,t,m_1,m_2)$ is GI, it is easy to show that Eq. (2.3) can be recast in the form

$$\begin{aligned} T(s,t,m_1,m_2) = {} & \hat{T}_1(t) + \hat{T}_2(t,m_1,m_2) \\ & + \hat{T}_3(s,t,m_1,m_2), \end{aligned} \tag{2.4}$$

where the $\hat{T}_i$ $(i = 1,2,3)$ are *separately* ξ independent. The propagatorlike parts of the vertex and box diagrams which enforce the gauge independence of $T_1(t)$ are called "pinch parts." The pinch parts emerge every time a gluon propagator or an elementary three-gluon vertex contribute a longitudinal k_μ to the original graph's numerator. The action of such a term is to trigger an elementary Ward identity of the form

$$\begin{aligned} k^\mu\gamma_\mu \equiv \not{k} &= (\not{k} + \not{p} - m_i) - (\not{p} - m_i) \\ &= S_i^{-1}(p+k) - S_i^{-1}(p), \end{aligned} \tag{2.5}$$

once it gets contracted with a γ matrix. The first term on the right-hand side of (2.5) will remove the internal fermion propagator, that is, a "pinch," whereas $S^{-1}(p)$ vanish on shell. Returning to the decomposition of Eq. (2.4), the function $\hat{T}_1$ is GI and may be identified with the contribution of the new propagator. We can construct the new propagator, or equivalently $\hat{T}_1$, directly from the Feynman rules. In doing so it is evident that any value for the gauge parameter ξ may be chosen, since $\hat{T}_1$, $\hat{T}_2$, and $\hat{T}_3$ are all independent of ξ. The simplest of all covariant gauges is certainly the Feynman gauge ($\xi = 1$), which removes the longitudinal part of the gluon propagator. Therefore the only possibility for pinching in four-fermion amplitudes arises from the four-momentum of the three-gluon vertices, and the only propagatorlike contributions come from vertex graphs and not from boxes.

The generalization of the PT from vectorlike theories (such as QCD) to the SM is technically and conceptually straightforward, as long as one assumes that the external fermionic currents are conserved. For example, applying the PT to a SM amplitude, such as $e^-\nu_e \to e^-\nu_e$, with $m_e = m_\nu = 0$, a ξ-independent self-energy for the W boson may be constructed [13].

The situation becomes more involved if one decides to consider nonconserved external fermionic currents, e.g., fermions with nonvanishing masses. The main reasons are the following.

(a) The charged W couples to fermions with different, nonvanishing masses $m_i, m_j \neq 0$, and consequently the elementary Ward identity of Eq. (2.5) gets modified to

$$\begin{aligned} k_\mu\gamma^\mu P_L \equiv \not{k}P_L = {} & S_i^{-1}(p+k)P_L - P_R S_j^{-1}(p) \\ & + m_i P_L - m_j P_R, \end{aligned} \tag{2.6}$$

where

$$P_{R,L} = \frac{1 \pm \gamma_5}{2} \tag{2.7}$$

are the chirality projection operators. The first two terms of Eq. (2.6) will pinch and vanish on shell, respectively, as they did before. But, in addition, a term proportional

to $m_i P_L - m_j P_R$ is left over. In a general R_ξ gauge such terms give rise to extra propagator and vertexlike contributions, not present in the massless case. For the neutral Z that couples to fermions of the same mass, we have to set $m_i = m_j = m$ in Eq. (2.6).

(b) Additional graphs involving the "unphysical" Goldstone bosons χ and ϕ and physical Higgs boson H, which do not couple to massless fermions, must now be included. Such graphs give rise to new pinch contributions, even in the Feynman gauge, as a result of the momenta carried by interaction vertices such as $\gamma\phi^+\phi^-$, $Z\phi^+\phi^-$, $W^+\phi^-\chi$, $HW^+\phi^-$, etc., e.g., vertices with one vector gauge boson and two scalar bosons. So, for example, all the graphs of Fig. 4 below, give rise to new vertexlike pinch contributions to the γWW and ZWW vertices, while in the massless case considered in [23] only graphs (1) and $R^{(1,2)}$ were present.

(c) After the pinch contributions have been identified, particular care is needed in deciding how to allot them among the (eventually ξ independent) quantities one is attempting to construct. When constructing GI TBV's, for example, in the massless case ($m_i = m_j = 0$), all vertexlike pinch contributions are allotted among the γWW and ZWW, the only two vertices which contribute to the amplitude. In the massive case we propose to study, vertices such as $\chi W^- W^+$, $HW^- W^+$, $Z\phi^- W^+$, etc., contribute nonvanishingly to the amplitude, and they must also be rendered GI through proper allocation of the available vertexlike pinch parts. The details of how this is accomplished will be presented in the next section.

Before we proceed with the construction of the vertices and the subtleties involved, we record some useful formulas. In what follows we use the Feynman rules and the conventions of [30]. The three-level vector-boson propagator $\Delta^i_{\mu\nu}(q)$ in the R_ξ gauges is given by

$$\Delta_i^{\mu\nu}(q,\xi_i) = \frac{1}{q^2 - M_i^2}\left[g^{\mu\nu} - (1-\xi_i)\frac{q^\mu q^\nu}{q^2 - \xi_i M_i^2}\right], \quad (2.8)$$

with $i = W, Z, \gamma$ and $M_\gamma = 0$. Its inverse $\Delta_i^{-1}(q,\xi_i)^{\mu\nu}$ is given by

$$\Delta_i^{-1}(q,\xi)^{\mu\nu} = (q^2 - M_i^2)g^{\mu\nu} - q^\mu q^\nu + \frac{1}{\xi_i} q^\mu q^\nu \ . \quad (2.9)$$

The propagators $\Delta_s(q,\xi_i)$ of the unphysical (would-be) Goldstone bosons are given by

$$\Delta_s(q,\xi_i) = \frac{-1}{q^2 - \xi_i M_i^2} \ , \quad (2.10)$$

with $(s,i) = (\phi, W)$ or (χ, Z) and explicitly depend on ξ_i. On the other hand, the propagators of the fermions (quarks and leptons) as well as the propagator of the physical Higgs particle are ξ_i independent at the tree level.

The following identities, which hold for *every* value of the gauge fixing parameters ξ_i, will be used extensively [21]:

$$\Delta_i^{\mu\nu}(q,\xi_i) = U_i^{\mu\nu}(q) - \frac{q^\mu q^\nu}{M_i^2}\Delta_s(q,\xi_i), \quad (2.11)$$

where

$$U_i^{\mu\nu}(q) = \left[g^{\mu\nu} - \frac{q^\mu q^\nu}{M_i^2}\right]\frac{1}{q^2 - M_i^2} \quad (2.12)$$

is the W and Z propagator in the unitary gauge ($\xi_W, \xi_Z \to \infty$) and

$$U_i^{-1}(q)^{\mu\nu} = g^{\mu\nu}(q^2 - M_i^2) - q^\mu q^\nu \quad (2.13)$$

its inverse. Furthermore,

$$\begin{aligned} g^\alpha_\nu &= \Delta^i_{\nu\mu}(q,\xi_i)\Delta_i^{-1}(q,\xi_i)^{\mu\alpha} \\ &= \Delta^i_{\nu\mu}(q,\xi_i)U_i^{-1}(q)^{\mu\alpha} - q_\nu q^\alpha \Delta_s(q,\xi_i) \end{aligned} \quad (2.14)$$

and

$$q^\mu = -M_i^2 q_\nu \Delta_i^{\nu\mu}(q,\xi_i) - q^2 q^\mu \Delta_s(q,\xi_i). \quad (2.15)$$

Finally, the divergences of the currents $J^\mu_Z, J^\mu_W, J^{+\mu}_W$ of [13] are related at the tree level to the currents of the would-be Goldstone bosons $J_\chi, J^-_\phi, J^+_\phi$ by the elementary identities

$$\begin{aligned} (\bar{e}\chi e) &= \frac{-iq^\nu}{M_Z}(\bar{e}Ze)_\nu, \\ (\bar{\nu}\phi^- e) &= \frac{-ip_2^\rho}{M_W}(\bar{\nu}W^- e)_\rho, \\ (\bar{e}\phi^+\nu) &= \frac{-ip_1^\sigma}{M_W}(\bar{e}W^+\nu)_\sigma, \end{aligned} \quad (2.16)$$

where q, p_1, and p_2 are the momenta carried by the bosons as shown in Fig. 2.

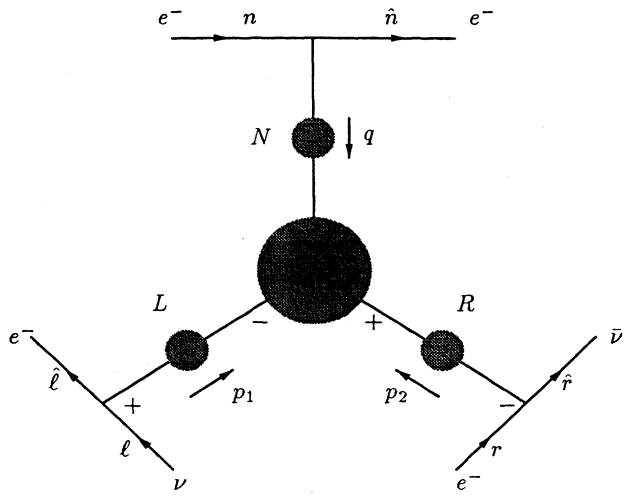

FIG. 2. General structure of the part $\hat{T}(q,p_1,p_2)$ of the S matrix that depends only on the momentum transfers q, p_1, p_2. The solid lines without orientation represent boson propagators.

III. GAUGE-INDEPENDENT THREE-BOSON VERTICES

In this section we show how to use the PT in order to construct gauge-invariant three-boson vertices (TBV's), with all three of their incoming momenta *off shell.*

We consider the S-matrix element for the process

$$e^-(n)+\nu(l)+e^-(r)\to e^-(\hat{n})+e^-(\hat{l})+\nu(\hat{r}), \quad (3.1)$$

where

$$q=n-\hat{n},\quad p_1=l-\hat{l},\quad p_2=r-\hat{r} \quad (3.2)$$

are the momentum transfers at the corresponding fermion lines; they represent the incoming momenta of each of the bosons, merging in the TBV's. The TBV's which can be extracted from the S-matrix element of the above process will be in general denoted as $\hat{\Gamma}^{NLR}$, with $N=\gamma,Z,\chi,H$, $L=W^-,\phi^-$, and $R=W^+,\phi^+$, where N, L, and R stand for the neutral, left (positive charge created), and right (positive charge destroyed) legs of the vertex.

We can extract GI *improper* vertices by identifying the part $\hat{T}(q,p_1,p_2)$ of the S matrix which is independent of the external momenta $n,r,l,\hat{n},\hat{r},\hat{l}$ and only depends on the momentum transfer q,p_1,p_2. The general form of $\hat{T}(q,p_1,p_2)$ is shown in Fig. 2. $\hat{T}(q,p_1,p_2)$ is GI as long as we append to the regular vertex graphs all parts of the rest of the graphs, which only depend on the momentum transfers q,p_1,p_2. Examples of graphs containing such vertexlike pinch parts are shown in Figs. 3(c) and 4.

The inclusion of these extra pieces cancels all ξ_i-dependent parts of the regular vertex diagrams; the only gauge dependence remaining stems from the tree-level expressions of the propagators of the boson legs. As we will see in Sec. V, the cancellation of this residual ξ_i dependence is enforced by a set of WI's satisfied by the GI $\hat{\Gamma}^{NLR}$'s. The final form of the GI $\hat{T}(q,p_1,p_2)$ is a sum of individually GI subamplitudes $\hat{T}^{NLR}(q,p_1,p_2)$ and is given by

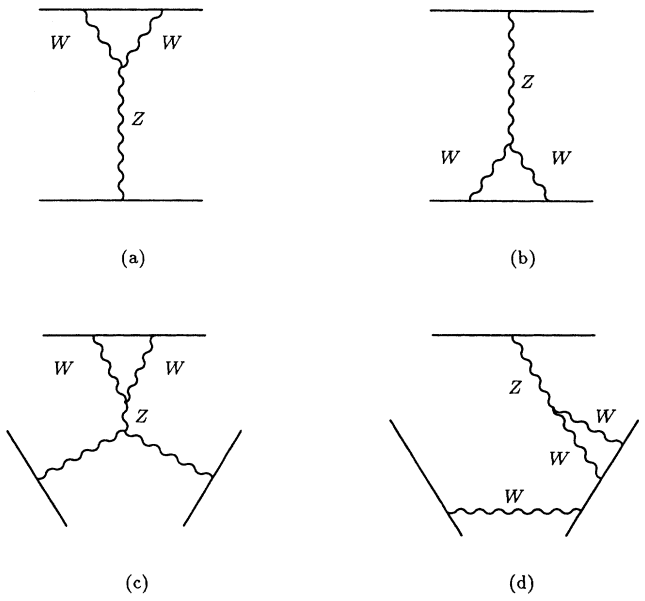

FIG. 3. Graphs contributing pinch parts to the construction of GI Z self-energies.

$$\begin{aligned}\hat{T}(q,p_1,p_2)&=\sum_{\{NLR\}}(\bar{e}Ne)(\bar{e}L\nu_e)(\bar{\nu}_eRe)\hat{T}^{NLR}(q,p_1,p_2)\\&=\sum_{\{NLR\}}(\bar{e}Ne)(\bar{e}L\nu_e)(\bar{\nu}_eRe)\hat{\Delta}_N(q)\hat{\Delta}_L(p_1)\hat{\Delta}_R(p_2)\hat{\Gamma}^{NLR}(q,p_1,p_2),\end{aligned} \quad (3.3)$$

where all internal Lorentz indices have been suppressed. In order to extract the proper $\hat{\Gamma}^{NLR}(q,p_1,p_2)$ from the respective $\hat{T}^{NLR}(q,p_1,p_2)$, one must strip off the three GI $\hat{\Delta}$'s, by multiplying $\hat{T}^{NLR}(q,p_1,p_2)$ with the respective inverse propagators $\hat{\Delta}^{-1}$. We remind the reader that the $\hat{\Delta}$ may be individually constructed through the application of the PT to appropriate four-fermion amplitudes (see, for example, [13] and [16]).

Another equivalent and more economical way to isolate the proper vertex, described in detail in [5] and [23], is to note that the conventional self-energies of the external boson legs can be converted to the respective GI PT self-energies, except for certain missing pinch pieces. These missing pieces may be supplemented to the self-energy by hand and correspondingly subtracted from the TBV's. All such terms are multiplied by an inverse tree-level propagator (which is the characteristic structure of all pinch terms), and they remove the tree-level boson propagator connecting them to the rest of the graph. Therefore they are effectively one-particle *irreducible*, and they may be freely added to the rest of the one-particle irreducible terms contributing to the TBV's [6].

Schematically, the GI TBV $\hat{\Gamma}_{NLR}$ will consist of the pieces

$$\hat{\Gamma}_{NLR}=\Gamma_{NLR}^{(\xi_i=1)}+\Gamma_{NLR}^{P}-\tfrac{1}{2}\Pi_{NN'}^{P}\Gamma_{N'LR}^{(0)}-\tfrac{1}{2}\Pi_{LL'}^{P}\Gamma_{NL'R}^{(0)}-\tfrac{1}{2}\Pi_{RR'}^{P}\Gamma_{NLR'}^{(0)}, \quad (3.4)$$

where $\Gamma_{NLR}^{(\xi_i=1)}$ are the conventional graphs contributing to the TBV in the Feynman gauge, Γ_{NLR}^{P} are all vertexlike pinch parts of box diagrams (also computed with $\xi_i=1$ [31]), which are kinematically equivalent to the TBV in question (this point will be further clarified later in this section), $\Gamma_{NLR}^{(0)}$ are tree-level expressions of respective TBV's,

and Π^P_{ij} $(i,j = N,L,R)$ is the pinch contribution to the ij-boson self-energy (again at $\xi_i = 1$). Since the derivation of the pinch parts of propagators has been extensively discussed in the literature, we will first focus on the technical details pertaining to the construction of the term Γ^P_{NLR} in Eq. (3.4).

The pinch parts of graphs are extracted using Eq. (2.6), whenever possible. The box diagrams of Fig. 4, for example, represent the complete set of diagrams that can contribute vertexlike parts to the γW^-W^+, ZW^-W^+, and χW^-W^+ vertices [32]. Depending on which of the internal fermion propagator has been removed, the vertexlike pinch amplitudes assume one of the following forms:

$$
\begin{aligned}
&(\bar{e}L\nu)\ldots(\bar{\nu}Re)\ldots\Delta^L_{\ldots}(p_1)\Delta^R_{\ldots}(p_2)\left[\frac{g^2}{2}(\bar{e}\gamma^\mu P_L e)B^N_{\ldots\mu}+\frac{g^2}{2}m_e(\bar{e}P_L e)\mathcal{M}^N_{\ldots}\right],\\
&(\bar{\nu}Re)\ldots(\bar{e}Ne)\ldots\Delta^R_{\ldots}(p_2)\Delta^N_{\ldots}(q)[(\bar{e}W^+\nu)^\mu B^L_{\ldots\mu}+iM_W(\bar{e}\phi^+\nu)\mathcal{M}^L_{\ldots}],\\
&(\bar{e}Ne)\ldots(\bar{e}L\nu)\ldots\Delta^N_{\ldots}(q)\Delta^L_{\ldots}(p_1)[(\bar{\nu}W^-e)^\mu B^R_{\ldots\mu}+iM_W(\bar{\nu}\phi^-e)\mathcal{M}^R_{\ldots}].
\end{aligned}
\tag{3.5}
$$

The ellipses in Eq. (3.5) represent appropriately contracted Lorentz indices, which we suppress. We note that the $\mathcal{M}$ terms originate from the mass leftovers of Eq. (2.6). The factors B and $\mathcal{M}$ in the expressions above are in general complicated functions of q, p_1, and p_2 and boson masses; however, they do not depend on the individual momenta and masses of the external "test" fermions. Note also that they are ultraviolet finite since they originated from box diagrams. Clearly, the B's or $\mathcal{M}$'s may be zero for some graphs. Once all relevant pinch contributions have been extracted, they must be judiciously allotted to the appropriate TBV's. To that end, one has to perform the following three steps.

(i) The couplings multiplying the B and $\mathcal{M}$ in the RHS of the first relation in Eq. (3.5) must be rewritten as a linear combination of the couplings of the bosons which can be attached to the corresponding fermion current. So for the couplings of the neutral bosons on the top fermion line we write

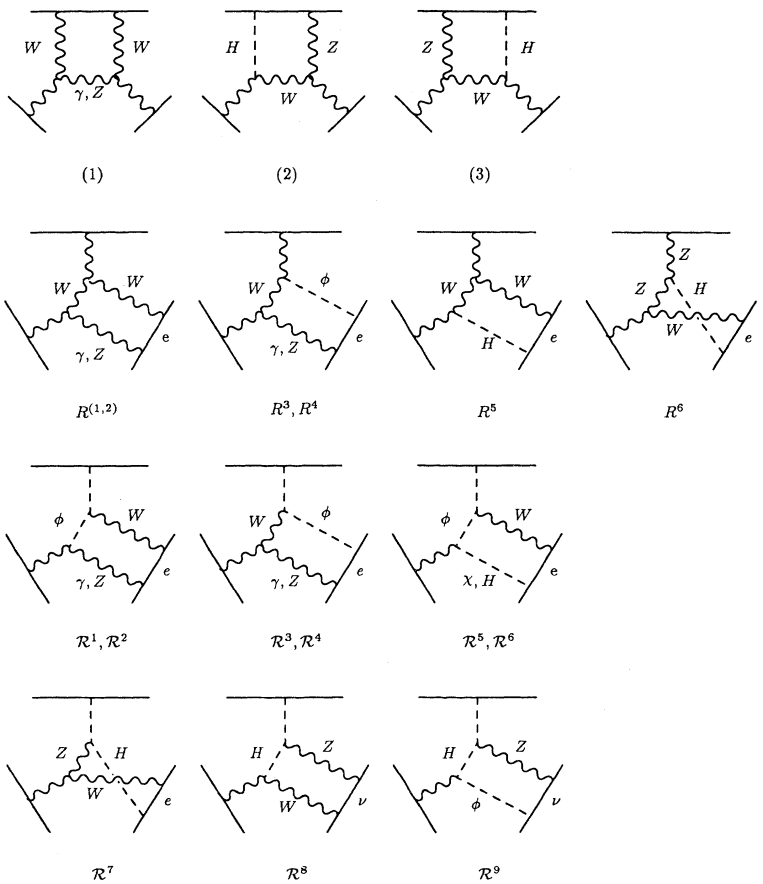

FIG. 4. Graphs providing pinch parts to the γWW, ZWW, and χWW vertices in the Feynman gauge. The diagrams pinching the left fermion line as well as all types of crossed diagrams are not shown.

$$\frac{g^2}{2}\gamma^\rho P_L = -gc(\bar{e}Ze)^\rho - gs(\bar{e}\gamma e)^\rho,$$
$$\frac{g^2}{2}m_e P_L = -gM_W(\bar{e}He) + gc\frac{iM_Z}{2}(\bar{e}\chi e). \tag{3.6}$$

On the other hand, the appropriate couplings for the charged bosons have already appears on the RHS of the second and third relations in Eq. (3.5).

(ii) We use the identities given in Eq. (2.16) to rewrite the couplings of the Goldstone bosons to the fermions as divergences of the corresponding currents of the gauge bosons. At the end of these two steps, the pinch parts in the square brackets of Eq. (3.5) assume the form

$$\left[-gc(\bar{e}Ze)^\rho\left(B^N_{\cdots\rho} - \frac{q_\rho}{2}\mathcal{M}^N_{\cdots}\right) - gs(\bar{e}\gamma e)^\rho B^N_{\cdots\mu} - gM_W(\bar{e}He)\mathcal{M}^N_{\cdots}\right], \tag{3.7}$$

$$[B^L_{\cdots\rho} + p_{1\rho}\mathcal{M}^L_{\cdots}](\bar{e}W^+\nu)^\rho, \tag{3.8}$$

$$[B^R_{\cdots\rho} + p_{2\rho}\mathcal{M}^R](\bar{\nu}W^-e)^\rho. \tag{3.9}$$

(iii) The final step in transforming these expressions into the desired form of TBV's is to recognize that a tree-level boson propagator must be attached at the point where the pinching took place. It is straightforward to make the missing photon and Higgs propagator appear. We only need to insert unity written as a product of a propagator and its inverse. The inverse propagator will be incorporated to the rest of the pinch expression. We emphasize that no additional ξ dependences are introduced into the pinch expressions through this process, since the part of the inverse photon propagator proportional to ξ_γ vanishes from the amplitude due to conservation of the electromagnetic current J^μ_γ, whereas the Higgs propagator and its inverse are GI at the tree-level. In order to accomplish this last step for the massive gauge bosons, we have to use the identities of Eq. (2.14), since now the relevant currents J^μ_Z and J^μ_W are not conserved. Finally, we obtain

$$(\bar{e}\gamma e)_\rho\frac{g^{\rho\nu}}{q^2}[-gsT^{\mu\nu}(q)B^N_{\cdots\mu}] + (\bar{e}He)\Delta_H(q)[-gM_W\Delta_H^{-1}(q)\mathcal{M}^N_{\cdots}]$$
$$+(\bar{e}Ze)_\rho\Delta^{\rho\nu}_Z(q)\left[-gcU^{-1}(q)_\nu{}^\mu{}_Z\left(B^N_{\cdots\mu} + \frac{q_\mu}{2}\mathcal{M}^N_{\cdots}\right)\right] + (\bar{e}\chi e)\Delta_\chi(q)\left[iM_Z gcq^\mu\left(B^N_{\cdots\mu} + \frac{q_\mu}{2}\mathcal{M}^N_{\cdots}\right)\right], \tag{3.10}$$

$$[B^L_{\cdots\mu} + p_{1\mu}\mathcal{M}^L_{\cdots}][U_W^{-1}(p_1)_\nu{}^\mu\Delta^{\rho\nu}_W(p_1,\xi_W)(\bar{e}W^+\nu)_\rho - iM_W p_1^\mu\Delta_\phi(p_1,\xi_W)(\bar{e}\phi^+\nu)], \tag{3.11}$$

$$[B^R_{\cdots\mu} + p_{2\mu}\mathcal{M}^R_{\cdots}][U_W^{-1}(p_2)_\nu{}^\mu\Delta^{\rho\nu}_W(p_2,\xi_W)(\bar{e}W^-\nu)_\rho - iM_W p_2^\mu\Delta_\phi(p_2,\xi_W)(\bar{e}\phi^-\nu)]. \tag{3.12}$$

It is now evident how the pinch parts must be allotted among the various (eventually GI) TBV's. We demonstrate it schematically below.

From the graphs that pinch at the top (neutral) fermion line [Eq. (3.10)], the pinch parts are distributed as follows

$$\begin{aligned}
-gsT_\nu{}^\mu(q)B^N_{\cdots\mu} &\to \hat{\Gamma}^{\gamma LR}_{\nu\cdots},\\
-gcU_Z^{-1}(q)_\nu{}^\mu\left(B^N_{\cdots\mu} + \frac{q_\mu}{2}\mathcal{M}^N_{\cdots}\right) &\to \hat{\Gamma}^{ZLR}_{\nu\cdots},\\
iM_Z gcq^\mu\left(B^N_{\cdots\mu} + \frac{q_\mu}{2}\mathcal{M}^N_{\cdots}\right) &\to \hat{\Gamma}^{\chi LR}_{\cdots},\\
-gM_W\Delta_H^{-1}(q)\mathcal{M}^N_{\cdots} &\to \hat{\Gamma}^{HLR}_{\cdots}.
\end{aligned} \tag{3.13}$$

From the graphs that pinch on the left [Eq. (3.11)], we have

$$\begin{aligned}
U_W^{-1}(p_1)_\nu{}^\mu(B^L_{\cdots\mu} - p_{1\mu}\mathcal{M}^L_{\cdots}) &\to \hat{\Gamma}^{NW^-R}_{\cdots\nu\cdots},\\
iM_W p_1^\mu(B^L_{\cdots\mu} - p_{1\mu}\mathcal{M}^L_{\cdots}) &\to \hat{\Gamma}^{N\phi^-R}_{\cdots},
\end{aligned} \tag{3.14}$$

and from the graphs that pinch on the right [Eq. (3.12)],

$$\begin{aligned}
U_W^{-1}(p_2)_\nu{}^\mu(B^R_{\cdots\mu} - p_{2\mu}\mathcal{M}^R_{\cdots}) &\to \hat{\Gamma}^{NLW^+}_{\cdots\nu},\\
iM_W p_2^\mu(B^R_{\cdots\mu} - p_{2\mu}\mathcal{M}^R_{\cdots}) &\to \hat{\Gamma}^{NL\phi^+}_{\cdots}.
\end{aligned} \tag{3.15}$$

The final step in the construction of the GI TVB's is the inclusion of all pinch terms that have been left over from converting gauge-dependent boson self-energies into their gauge-independent PT counterparts at other parts of the amplitude considered; they constitute the third term on the RHS of Eq. (3.4). To begin with, it is important to recognize that in addition to the boson legs at-

tached to the TBV's, the boson legs of the "monodromic" graphs [collectively depicted in Figs. 8(e), 8(f), 8(g), below] must be rendered GI. We call them "monodromic" (one-way), because their graph structure of vertices and edges (propagators) is that of a "Eulerian-path" or self-avoiding curve. That is, all the vertices can be visited by a line that does not run through an edge twice. Note that they contain an off-shell fermion propagator. In the rest of this section, we outline how such pieces are included in the vertices through a specific example.

Let us concentrate on the Z self-energy legs. In the Feynman gauge ($\xi_i = 1$), the only propagatorlike pinch parts for the GI Z self-energy originate from the graph shown in Fig. 3(a) and its mirror graph Fig. 3(b) and their contribution is equal. For the Z self-energy leg attached to the ZWW vertex, one of the above graphs [Fig. 3(c)], is already present in the amplitude we consider and supplies half of the necessary pinch contribution. The other half, where the pinch would occur at the side where we now have the TBV, is missing. Therefore its pinch contribution must be supplemented by hand to the Z self-energy graphs and subsequently subtracted from the ZWW vertex graphs. We observe that this contribution to the vertex will be of the form $-2g^2c^2 I_{WW}(q)[U_Z^{\mu\nu}(q)]^{-1}\Delta_Z^{\nu\rho}(q,\xi_Z)\Gamma^{ZWW}_{\rho\alpha\beta}$. This last expression is explicitly gauge dependent. The effect of the monodromic graphs is to precisely cancel this residual gauge dependence. To understand how this cancellation mechanism works, we now concentrate on the vertexlike pieces originating from the monodromic graphs. As a first step, their bosonic legs must be rendered GI; in doing so, we note that, unlike the previous case, all the necessary propagatorlike pinch parts are now available [an example of a graph that contributes such a pinch term is shown in Fig. 3(d)]. One then proceeds as usually and first pinches the fermion propagator inside the loop and then uses Eqs. (2.14) and (2.15) to attach boson propagators at the point where the pinching took place. At this point one observes that the momenta accompanying the part with the scalar propagator Δ_s in Eqs. (2.14), (2.15) can trigger additional pinching and remove the remaining fermion propagator that was outside of the loop. Thus a vertexlike piece finally emerges from this part and must be included with the rest of the vertex graphs. Clearly, all these pieces are also explicitly gauge dependent since they carry a $\Delta_\chi(q,\xi_Z)$ and, by using Eq. (2.11) exactly, cancel against the relevant $\Delta_\chi(q,\xi_Z)$ part coming from the leg attached to the TBV. In the remaining expression the tree-level propagators in the unitary gauge also cancel and the part that needs to be appended to the ZWW vertex is $-2g^2c^2 I_{WW}(q)\Gamma^{ZWW}_{\mu\alpha\beta}$. A similar procedure must be followed case by case for all the TBV's and will conclude the construction of a GI three-boson vertex.

IV. VERTICES γW^-W^+, ZW^-W^+, χW^-W^+

In the previous section we presented the general procedure for constructing GI TBV's via the PT. In this section we focus on three particular TBV's, namely, $\hat{\Gamma}^{\gamma W^-W^+}$, $\hat{\Gamma}^{ZW^-W^+}$, and $\hat{\Gamma}^{\chi W^-W^+}$, and we describe in detail their derivation. This section is rather technical; we present several intermediate results, which will also be used in subsequent sections. The final expressions for $\hat{\Gamma}^{\gamma W^-W^+}_{\mu\alpha\beta}$, $\hat{\Gamma}^{ZW^-W^+}_{\mu\alpha\beta}$, and $\hat{\Gamma}^{\chi W^-W^+}_{\alpha\beta}$ are summarized in Eqs. (4.33)–(4.35).

We adopt the following convention. The scalar parts of boson propagators of mass M_A and momentum q will be denoted by

$$A(q) \equiv \frac{1}{q^2 - M_A^2}. \tag{4.1}$$

For example, with this notation the tree-level propagator for the W in Eq. (2.8) assumes the form

$$\Delta_W^{\mu\nu}(q) = \left[g^{\mu\nu} - (1-\xi_i)\frac{q^\mu q^\nu}{q^2 - \xi_i M_i^2}\right] W(q). \tag{4.2}$$

We introduce the shorthand notation

$$\int (ABC)\{\cdots\} \equiv \int (dk) A(k+p_1)B(k-p_2)C(k)\{\cdots\}, \tag{4.3}$$

where the momentum integration measure is $(dk) = \frac{d^4k}{i(2\pi)^4}$ for convergent integrals and $(dk) = \mu^{4-n}\frac{d^nk}{i(2\pi)^n}$ for dimensionally regularized integrals. Furthermore, we define the scalar integrals

$$J_{ABC} \equiv J_{ABC}(q,p_1,p_2) = \int (ABC), \tag{4.4}$$

$$I_{AB}(q) = \int (dk) A(k) B(k+q). \tag{4.5}$$

The box diagrams containing vertexlike contributions, in the Feynman gauge, are shown in Fig. 4. From the first two diagrams of Fig. 4, which we treat as one, we obtain

$$N^1_{\nu\alpha\beta} = gcU_Z^{-1}(q)^\rho_\mu g^2 B_{\rho\alpha\beta} \tag{4.6}$$

and

$$\mathcal{N}^1_{\alpha\beta} = -iM_Z gcq^\rho g^2 B_{\rho\alpha\beta}, \tag{4.7}$$

where $g^2 B_{\rho\alpha\beta}$ is the same expression as in the case for conserved currents [see [23], Eqs. (3.5) and (3.6)]; namely,

$$g^2 B_{\rho\alpha\beta} = \sum_{V=\gamma,Z} g_V^2 \int (WWV)\Big\{ g_{\alpha\beta}[k - \tfrac{3}{2}(p_1-p_2)]_\mu - g_{\alpha\mu}(3k+2q)_\beta - g_{\beta\mu}(3k-2q)_\alpha \Big\}, \tag{4.8}$$

with $g_\gamma = gs$ and $g_Z = gc$. $N^1_{\mu\alpha\beta}$ is allotted to the vertex $\hat{\Gamma}^{ZW^-W^+}_{\mu\alpha\beta}$ whereas $\mathcal{N}^1_{\alpha\beta}$ to $\hat{\Gamma}^{\chi W^-W^+}_{\alpha\beta}$.

Similarly, the graphs containing a Higgs boson (2 and 3 in Fig. 4) yield

$$N^2_{\mu\alpha\beta} + N^3_{\mu\alpha\beta} = -M_Z^2 g^3 c q_\mu g_{\alpha\beta} \mathcal{M} \tag{4.9}$$

and

$$\mathcal{N}^2_{\alpha\beta} + \mathcal{N}^3_{\alpha\beta} = -iM_Z q^2 g^3 c g_{\alpha\beta} \mathcal{M}, \tag{4.10}$$

with

$$\mathcal{M} = \tfrac{1}{2}(J_{HZW} + J_{ZHW}). \tag{4.11}$$

We note that box diagrams which contain any two internal neutral bosons, except the Higgs boson, give a zero total pinch contribution. This is so because the pinch parts of the direct diagrams cancel against the corresponding pinch parts of the crossed diagram. Similarly, the pinch contributions of diagrams with one ϕ and one W in the loop cancel against the corresponding contribution from the mirror graphs, e.g., $W \leftrightarrow \phi$.

The pinch contributions of the diagrams 1–6 of the second row of Fig. 4, where the pinching occurs at the leg of the W^+, are extracted following exactly similar steps. We denote these pinch contributions by $R^i_{\mu\alpha\beta}$ where $i = 1, \ldots, 6$. In what follows the suffix "cr" is used to denote the inclusion of the crossed graphs which are not shown in Fig. 4. The relevant expressions of the pinch contributions of these graphs are

$$R^{(1,2,2\mathrm{cr})}_{\mu\alpha\beta} = gcU_W^{-1}(p_2)^\rho_\beta g^2 B^-_{\mu\alpha\beta} + R^1_{\mu\alpha\beta} + R^2_{\mu\alpha\beta}, \tag{4.12}$$

where

$$\begin{aligned} R^1_{\mu\alpha\beta} &= g^3 c s^2 M_W^2 p_{2\beta} q_{\mu\alpha} J_{WW\gamma}, \\ R^2_{\mu\alpha\beta} &= g^3 c \left(\frac{1-2s^2}{2}\right) M_W^2 p_{2\beta} g_{\mu\alpha} J_{WWZ} \end{aligned} \tag{4.13}$$

and

$$g^2 B^-_{\mu\alpha\beta}(q, p_1, p_2) = \sum_{V=\gamma,Z} g_V^2 \int (WWV) G_{\mu\alpha\beta}(q, p_1, p_2), \tag{4.14}$$

with

$$\begin{aligned} G_{\mu\alpha\beta}(q, p_1, p_2) = {} & g_{\alpha\beta}(3k + 3p_1 - 2p_2)_\mu \\ & + g_{\mu\beta}(3k + p_1 - 2q)_\alpha \\ & - g_{\alpha\mu}(k + 2p_1 - 2q)_\beta. \end{aligned} \tag{4.15}$$

Note that the result of the conserved current case can be recovered from Eq. (4.14) if we neglect the terms proportional to $p_{1\alpha}$ and $p_{2\beta}$ [Eq. (3.11) of [23]].

The rest of the diagrams give

$$R^3_{\mu\alpha\beta} = g^3 \frac{s^4}{c} M_W^2 p_{2\beta} g_{\mu\alpha} J_{WW\gamma}, \tag{4.16}$$

$$R^4_{\mu\alpha\beta} + R^{4\mathrm{cr}}_{\mu\alpha\beta} = g^3 \frac{s^2(1-2s^2)}{2c} M_W^2 p_{2\beta} g_{\mu\alpha}, J_{WWZ}\ , \tag{4.17}$$

$$R^5_{\mu\alpha\beta} = \frac{g^3 c M_W^2}{2} p_{2\beta} g_{\mu\alpha} J_{WWH}, \tag{4.18}$$

$$R^6_{\mu\alpha\beta} = \frac{g^3 M_W^2}{2c} p_{2\beta} g_{\mu\alpha} J_{ZHW}. \tag{4.19}$$

We next turn to the rest of the graphs of Fig. 4, third and fourth rows, and isolate the pinch contributions, which will be appended to the vertex $\hat{\Gamma}^{\chi W^- W^+}_{\alpha\beta}$. We denote them by $\mathcal{R}^i_{\alpha\beta}$ where $i = 1, \ldots, 9$. Their explicit expressions are

$$\mathcal{R}^1_{\alpha\beta} + \mathcal{R}^2_{\alpha\beta} + \mathcal{R}^{2\mathrm{cr}}_{\alpha\beta} = \frac{g^3}{iM_Z} \frac{s^2}{2c} M_W^2 U_W^{-1}(p_2)_{\alpha\beta} \sum_{V=\gamma,Z} b_V J_{WWV}, \tag{4.20}$$

$$\mathcal{R}^3_{\alpha\beta} = \frac{g^3}{iM_Z} \frac{s^2}{2c} M_W^2 p_{2\beta} \int (WW\gamma)(k-2q)_\alpha, \tag{4.21}$$

$$\mathcal{R}^4_{\alpha\beta} + \mathcal{R}^{4\mathrm{cr}}_{\alpha\beta} + \mathcal{R}^5_{\alpha\beta} = \frac{g^3}{iM_Z} \frac{cM_W^2}{2} p_{2\beta} \int (WWZ) k_\alpha - \frac{g^3}{iM_Z} \frac{1-s^2}{2c} M_W^2 p_{2\beta} q_\alpha J_{WWZ} + \frac{g^3 M_W^2}{i8cM_Z} p_{1\alpha} p_{2\beta} J_{WWZ}. \tag{4.22}$$

The last term on the RHS of Eq. (4.22) cancels against the corresponding contribution from the left, coming from the graphs $\mathcal{L}^4_{\alpha\beta} + \mathcal{L}^{4\mathrm{cr}}_{\alpha\beta} + \mathcal{L}^5_{\alpha\beta}$.

$$\mathcal{R}^6_{\alpha\beta} = \frac{g^3}{iM_Z} \frac{M_W^2}{4c} p_{2\beta} \int (WWH) k_\alpha, \tag{4.23}$$

$$\mathcal{R}^7_{\alpha\beta} = -\frac{g^3}{iM_Z} \frac{M_W^2}{2c} q_\alpha p_{2\beta} J_{ZHW}, \tag{4.24}$$

$$\mathcal{R}^8_{\alpha\beta} + \mathcal{R}^{8\mathrm{cr}}_{\alpha\beta} = \frac{g^3}{iM_Z} \frac{M_W^2}{2c} U_W^{-1}(p_2)_{\alpha\beta} J_{HZW}, \tag{4.25}$$

$$\mathcal{R}^{9}_{\alpha\beta} + \mathcal{R}^{9\mathrm{cr}}_{\alpha\beta} = \frac{g^3}{iM_Z}\frac{(1-2s^2)}{4c} M_Z^2 p_{2\beta} \int (HZW)(2k+p_1)_\alpha. \tag{4.26}$$

The corresponding diagrams where the pinching occurs at the left fermion line we will denote as $L^i_{\mu\rho\beta}$ and $\mathcal{L}^i_{\rho\beta}$, respectively. (These diagrams are not shown.) They are given by

$$L^i_{\mu\alpha\beta}(q,p_1,p_2) = -R^i_{\mu\beta\alpha}(q,p_2,p_1), \quad \mathcal{L}^i_{\alpha\beta}(q,p_1,p_2) = -\mathcal{R}^i_{\beta\alpha}(q,p_2,p_1). \tag{4.27}$$

The total pinch contribution is the sum of all relevant terms. We define

$$\sum_{i=1}^{6} R^i_{\mu\alpha\beta} = g^3 c M_W^2 p_{2\beta} g_{\mu\alpha} \mathcal{M}^-, \quad \sum_{i=1}^{6} L^i_{\mu\alpha\beta} = g^3 c M_W^2 p_{1\alpha} g_{\mu\beta} \mathcal{M}^+, \tag{4.28}$$

$$\sum_{i=1}^{9} \mathcal{R}^i_{\alpha\beta} = \frac{g^3 c}{iM_Z} \mathcal{R}^-_{\alpha\beta}, \quad \sum_{i=1}^{6} \mathcal{L}^i_{\alpha\beta} = \frac{g^3 c}{iM_Z} \mathcal{L}^+_{\alpha\beta}, \tag{4.29}$$

where crossed graphs are included in the sums and

$$\mathcal{M}^-(q,p_1,p_2) = \frac{s^2}{c^2} J_{WW\gamma} + \frac{1-2s^2}{2c^2} J_{WWZ} + \frac{1}{2} J_{WWH} + \frac{1}{2c^2} J_{ZHW}, \tag{4.30}$$

$$\mathcal{M}^+(q,p_1,p_2) = -\mathcal{M}^-(q,p_2,p_1). \tag{4.31}$$

The last step is to add the pinch contributions to the regular vertex graphs. Thus, if we define

$$g^2 g_V \Gamma^{VW^-W^+}_{\mu\alpha\beta}|_{\xi_i=1} = \sum_{i=1}^{n_V} V^i_{\mu\alpha\beta}|_{\xi_i=1}, \quad g^3 c \Gamma^{\chi W^- W^+}_{\alpha\beta}|_{\xi_i=1} = \sum_{i=1}^{21} \mathcal{S}^i_{\alpha\beta}|_{\xi_i=1} \tag{4.32}$$

to be the sum of the usual graphs of the respective vertices in the Feynman gauge (depicted, respectively, in Fig. 5, with $V = \gamma, Z$, $n_\gamma = 28$, $n_Z = 34$ and Fig. 6), we arrive at the following expressions for the GI TBV's:

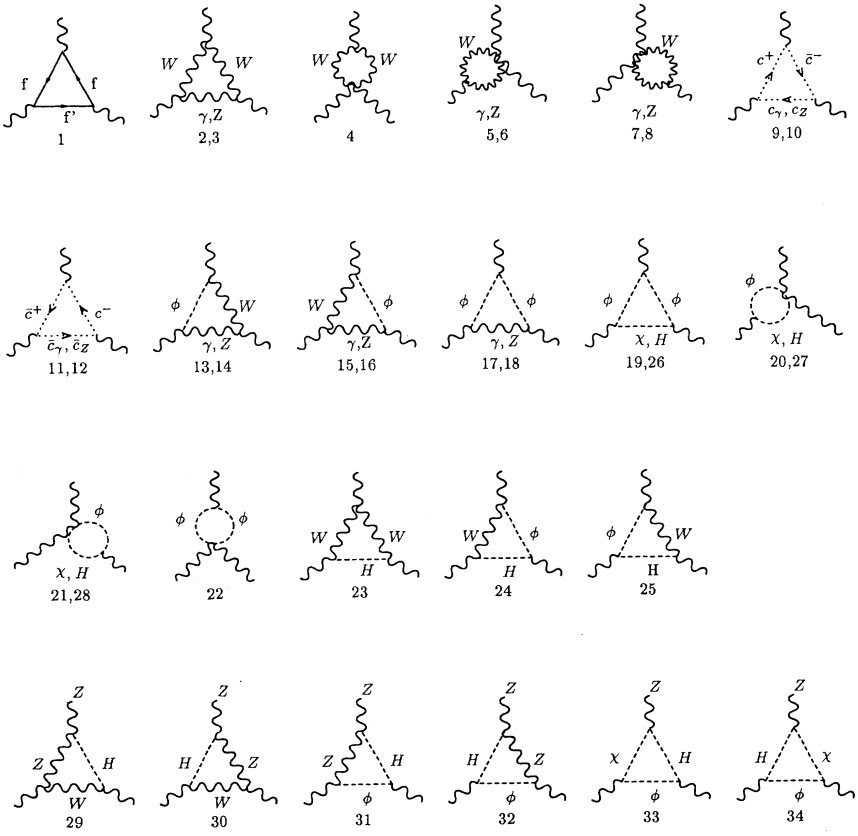

FIG. 5. Usual graphs contributing to the γWW and ZWW vertices in the Feynman gauge. Their corresponding expressions are denoted as $V^i_{\mu\alpha\beta}$ in the text. In the unitary gauge only the graphs (1)–(8), (23), (29), and (30) are present; they are denoted as $\mathcal{V}^i_{\mu\alpha\beta}$. In the context of the BFM, additional graphs must be included.

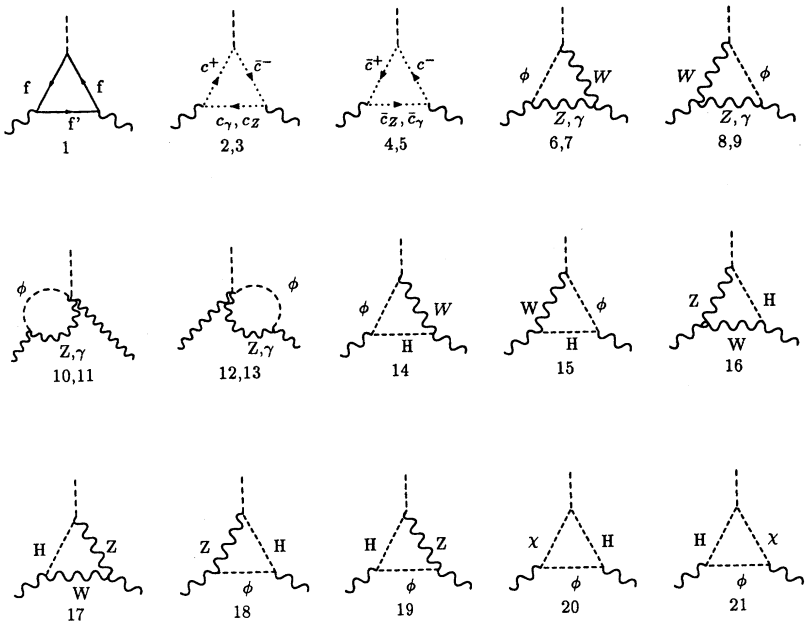

FIG. 6. Usual graphs contributing to the χWW vertex in the Feynman gauge. In the text they are denoted as $S^i_{\mu\alpha\beta}$. None of these graphs exist in the unitary gauge. In the BFM additional graphs must be included, whereas graphs containing ghosts are absent.

$$\frac{1}{g^3 s}\hat{\Gamma}^{\gamma W^- W^+}_{\mu\alpha\beta} = \Gamma^{\gamma W^- W^+}_{\mu\alpha\beta}|_{\xi_i=1} + q^2 T(q)^\rho_\mu B_{\rho\alpha\beta} + U_W^{-1}(p_1)^\rho_\alpha B^+_{\mu\rho\beta} + U_W^{-1}(p_2)^\rho_\beta B^-_{\mu\alpha\rho}$$
$$-2\Gamma_{\mu\alpha\beta}[I_{WW}(q) + s^2 I_{W\gamma}(p_1) + c^2 I_{WZ}(p_1) + s^2 I_{W\gamma}(p_2) + c^2 I_{WZ}(p_2)]$$
$$+p_{2\beta} g_{\mu\alpha}\mathcal{M}^- + p_{1\alpha} g_{\mu\beta}\mathcal{M}^+, \tag{4.33}$$

$$\frac{1}{g^3 c}\hat{\Gamma}^{ZW^- W^+}_{\mu\alpha\beta} = \Gamma^{ZW^- W^+}_{\mu\alpha\beta}|_{\xi_i=1} + U_Z^{-1}(q)^\rho_\mu B_{\rho\alpha\beta} + U_W^{-1}(p_1)^\rho_\alpha B^+_{\mu\rho\beta} + U_W^{-1}(p_2)^\rho_\beta B^-_{\mu\alpha\rho}$$
$$-2\Gamma_{\mu\alpha\beta}[I_{WW}(q) + s^2 I_{W\gamma}(p_1) + c^2 I_{WZ}(p_1) + s^2 I_{W\gamma}(p_2) + c^2 I_{WZ}(p_2)]$$
$$+q_\mu g_{\alpha\beta} M_Z^2 \mathcal{M} + p_{2\beta} g_{\mu\alpha} M_W^2 \mathcal{M}^- + p_{1\alpha} g_{\mu\beta} M_W^2 \mathcal{M}^+, \tag{4.34}$$

$$\frac{1}{g^3 c}\hat{\Gamma}^{\chi W^- W^+}_{\alpha\beta} = \Gamma^{\chi W^- W^+}_{\alpha\beta}|_{\xi_i=1} - iM_Z q^\rho B_{\rho\alpha\beta} - iM_Z q^2 \mathcal{M} - \frac{i}{M_Z}\mathcal{R}^-_{\alpha\beta} - \frac{i}{M_Z}\mathcal{L}^+_{\alpha\beta}. \tag{4.35}$$

V. WARD IDENTITIES

In the previous two sections we outlined the construction of a generic GI TBV and we computed the exact one-loop closed forms for the GI $\hat{\Gamma}^{\gamma W^- W^+}_{\mu\alpha\beta}$, $\hat{\Gamma}^{ZW^- W^+}_{\mu\alpha\beta}$, $\hat{\Gamma}^{\chi W^- W^+}_{\alpha\beta}$. In this section we proceed to derive a set of Ward identities that the GI TBV's satisfy. These Ward identities are a direct consequence of the gauge independence of the S matrix order by order in perturbation theory. It should be emphasized that the derivation of the WI's does not require knowledge of the explicit closed form of the TBV's involved.

After the construction of GI TBV's has been completed, the amplitude we consider has been reorganized into individually ξ-independent structures connected by ξ-dependent tree-level propagators. In other words, the PT algorithm only cancels all ξ dependences originating from the tree-level propagators appearing *inside* the loops, but a residual ξ dependence, stemming from boson propagators outside of loops, survives at the end of the pinching process. The cancellation of this last ξ dependence becomes possible due to a set of WI's satisfied by the GI TBV. One can actually derive these WI's *without* any detailed knowledge of the algorithm which gives rise to the GI TBV. All one needs to assume is that such an algorithm exists (in our case the PT algorithm) and that all residual ξ dependences should cancel from the S matrix. So once the GI TBV's have been constructed, one should examine whether or not they actually satisfy the required WI's, as a self-consistency check. In this section we use the above arguments to derive the WI's and we will explicitly check their validity at one loop in the next section.

It is instructive to illustrate the derivation of WI's for a simpler case, namely, the GI W propagator. We consider the one-loop S-matrix element of the process

$$e^-(b) + \nu_e(t) \to \nu_e(\hat{b}) + e^-(\hat{t}), \tag{5.1}$$

with $q = t - \hat{t} = \hat{b} - b$, and apply the PT rules. As shown in Fig. 7, the part of the S matrix which only depends on q^2 assumes the form

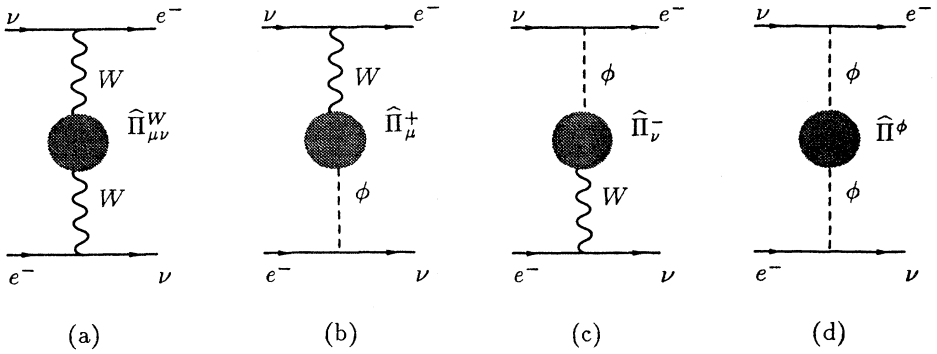

FIG. 7. GI self-energies $\hat{\Pi}^W_{\mu\nu}$, $\hat{\Pi}^+_\mu$, $\hat{\Pi}^-_\nu$, and $\hat{\Pi}^\phi$ [(a), (b), (c), and (d), respectively].

$$\hat{T}_1 = (\bar{e}W^+\nu)_\rho \Delta_W^{\rho\mu} \hat{\Pi}^W_{\mu\nu} \Delta_W^{\nu\sigma} (\bar{\nu}W^-e)_\sigma + (\bar{e}W^+\nu)_\rho \Delta_W^{\rho\mu} \hat{\Pi}^+_\mu \Delta_\phi (\bar{\nu}\phi^- e)$$
$$+ (\bar{e}\phi^+\nu)\Delta_\phi \hat{\Pi}^-_\mu \Delta_W^{\nu\sigma} (\bar{\nu}W^-e)_\sigma + (\bar{e}\phi^+\nu)\Delta_\phi \hat{\Pi}^\phi \Delta_\phi (\bar{\nu}\phi^- e). \tag{5.2}$$

Using Eq. (2.16) in order to pull out the factor $(\bar{e}W^+\nu)_\rho(\bar{\nu}W^-e)_\sigma$, as well as Eq. (2.14), we can cast the above expression in the form

$$\hat{T}_1 = (\bar{e}W^+\nu)_\rho \Bigg[\left(U_W^{\rho\mu} - \frac{q^\rho q^\mu}{M_W^2}\Delta_\phi \right) \hat{\Pi}^W_{\mu\nu} \left(U_W^{\nu\sigma} - \frac{q^\nu q^\sigma}{M_W^2}\Delta_\phi \right) + \frac{(-iq^\rho)}{M_W}\Delta_\phi \hat{\Pi}^\phi \Delta_\phi \frac{iq^\sigma}{M_W}$$
$$+ \left(U_W^{\rho\mu} - \frac{q^\rho q^\mu}{M_W^2}\Delta_\phi \right) \hat{\Pi}^+_\mu \Delta_\phi \frac{iq^\sigma}{M_W} + \frac{(-iq^\rho)}{M_W}\Delta_\phi \hat{\Pi}^W_{\mu\nu} \left(U_W^{\nu\sigma} - \frac{q^\nu q^\sigma}{M_W^2}\Delta_\phi \right) \Bigg] (\bar{\nu}W^-e)_\sigma. \tag{5.3}$$

In this last expression the ξ dependence is carried solely by the tree-level Goldstone boson propagators $\Delta_\phi(q, \xi_W)$. The requirement that $\hat{T}_1$ be ξ independent gives rise to two independent equations; the first enforces the cancellation of the terms with only one Δ_ϕ factor, whereas the second enforces the cancellation of the terms with a $\Delta_\phi\Delta_\phi$ factor. It is then a matter of simple algebra to show that the following WI's should hold [33]:

$$q^\mu \hat{\Pi}^W_{\mu\nu}(q) \mp iM_W \hat{\Pi}^\pm_\nu(q) = 0, \tag{5.4}$$

$$q^\mu \hat{\Pi}^\pm_\mu(q) \pm iM_W \hat{\Pi}^\phi(q) = 0, \tag{5.5}$$

$$q^\mu q^\nu \hat{\Pi}^W_{\mu\nu}(q) - M_W^2 \hat{\Pi}^\phi(q) = 0. \tag{5.6}$$

Similarly, the requirement of gauge independence for the S-matrix element of a neutral current process gives rise to the following set of WI's, relating the two-point Green's functions of Z and its Goldstone boson χ:

$$q^\mu \hat{\Pi}^Z_{\mu\nu}(q) - iM_Z \hat{\Pi}^{Z\chi}_\nu(q) = 0, \tag{5.7}$$

$$q^\mu \hat{\Pi}^{Z\chi}_\mu(q) + iM_Z \hat{\Pi}^\chi(q) = 0, \tag{5.8}$$

$$q^\mu q^\nu \hat{\Pi}^Z_{\mu\nu}(q) - M_Z^2 \hat{\Pi}^\chi(q) = 0. \tag{5.9}$$

We now turn to our main objective, namely, the derivation of the WI's for the GI TBV's. We consider again the S matrix element of the process in Eq. (3.1). After the pinching is performed, we focus on the diagrams of Fig. 8, where now the "blobs" represent GI expressions. As before, the residual ξ dependence of these graphs enters only through the tree-level bosonic propagators (solid, not-oriented lines). We call these graphs, respectively, (i) three-boson vertex graphs [Fig. 8(a)], (ii) self-energy graphs [Figs. 8(b), 8(c), 8(d)], and (iii) monodromic graphs [Figs. 8(e), 8(f), 8(g)] [34].

At first sight, the monodromic graphs do not appear to be akin to the graphs of types (i) and (ii) (which only depend on the momentum transfers q, p_1, p_2), since they seem to explicitly depend on the external fermion momenta n, l, r or $\hat{n}, \hat{l}, \hat{r}$ through the internal off-shell fermion propagators. Equivalently, one might think that the characteristic factor $(\bar{e}Ne)(\bar{E}L\nu_e)(\bar{\nu}_e Re)$, containing the external fermionic currents, cannot be pulled out from the monodromic graphs. One should note, however, that in the monodromic graphs additional pinching can take place, triggered by the longitudinal part of the bare vector boson propagators, thus eliminating the dependence on the internal fermion propagator. These pinch parts are vertexlike and will therefore combine with the graphs of (i) and (ii) in order to cancel the remaining gauge dependence from the amplitude.

To demonstrate this final cancellation, we use again Eq. (2.11) in order to isolate the residual gauge dependence of the S matrix into bare Goldstone boson propagators only. All gauge-dependent terms will display a characteristic structure, depending on the number and kind of Goldstone boson propagators they contain and the momenta they carry. Clearly, all such terms form linearly independent combinations. A term with

a gauge dependence of the form $\Delta_\chi(q,\xi_Z)\Delta_\phi(p_1,\xi_W)$, for example, cannot cancel against a term of the form $\Delta_\phi(p_2,\xi_W)\Delta_\phi(p_1,\xi_W)$, nor a term of the form $\Delta_\chi(q,\xi_Z)\Delta_\phi(p_2,\xi_W)$. Therefore, for the final cancellation to occur, the cofactors in front of all such linearly independent terms must individually vanish. This last condition gives rise to the aforementioned WI's.

Let us first look at terms carrying only a gauge-dependent factor of $\Delta_\chi(q,\xi_Z)$. Such terms can arise only from the diagrams shown in Fig. 9. In what follows we use the WI's of the boson self-energies Eqs. (5.4)–(5.9) as well as the WI's of the tree-level three-vector-boson vertex

$$q^\mu\Gamma^{VW^-W^+}_{\mu\alpha\beta}(q,p_1,p_2)=g_V[U_W^{-1}(p_2)_{\alpha\beta}-U_W^{-1}(p_1)_{\alpha\beta}] \tag{5.10}$$

and pull out the common factor $(\bar{e}Ze)_\nu(\bar{\nu}W^+e)_\rho(\bar{e}W^-\nu)_\sigma$. Then the $\Delta_\chi(q,\xi_Z)$ gauge-dependent part is given by

$$\frac{1}{M_Z^2}\Delta_\chi(q,\xi_Z)\{C_v+C_{se}+C_m^P\}^{\nu\rho\sigma}, \tag{5.11}$$

where C_v, C_{se}, and C_m^P are the contributions of the vertex, self-energy, and the pinched monodromic graphs, respectively:

$$C_v^{\nu\rho\sigma}=U_W^{\alpha\rho}(1)U_W^{\beta\sigma}(2)q^\nu[q^\mu\hat{\Gamma}^W_{\mu\alpha\beta}+iM_W\hat{\Gamma}^\zeta_{\alpha\beta}], \tag{5.12}$$

$$C_{se}^{\nu\rho\sigma}=-U_W^{\alpha\rho}(1)U_W^{\beta\sigma}(2)q^\nu gc[\hat{\Pi}^W_{\alpha\beta}(1)-\hat{\Pi}^W_{\alpha\beta}(2)]-gcH^{\nu\rho\sigma}, \tag{5.13}$$

$$(C_m^P)^{\nu\rho\sigma}=gcH^{\nu\rho\sigma}, \tag{5.14}$$

with

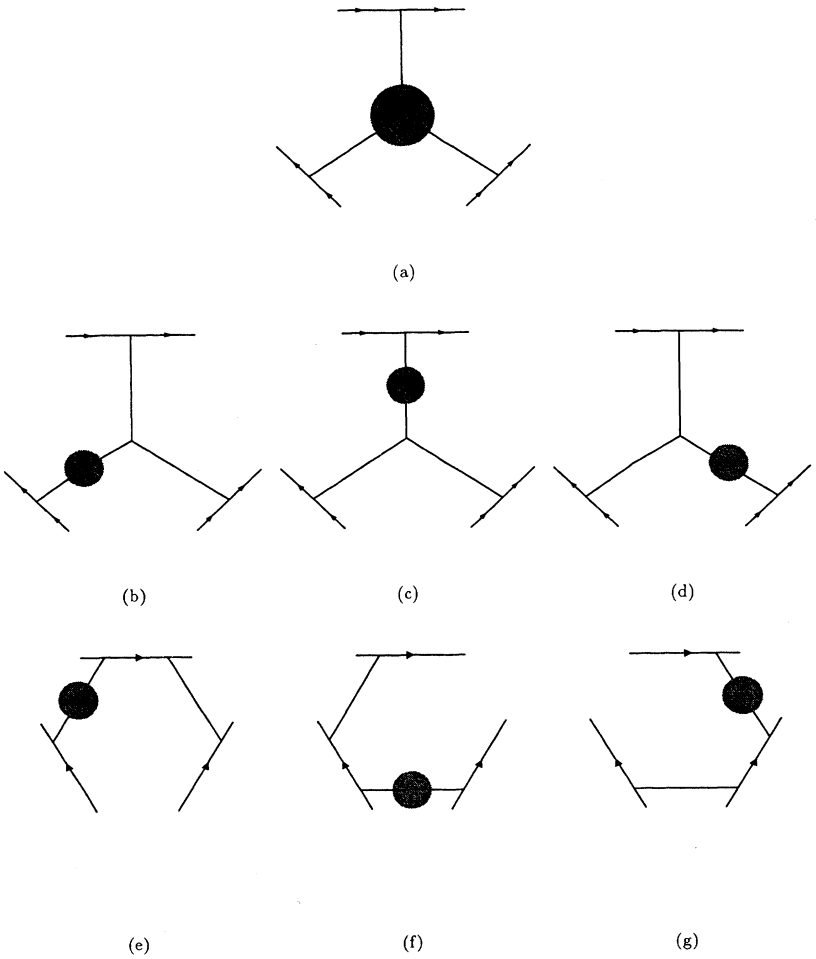

FIG. 8. Vertex, self-energy, and monodromic graphs of the S matrix for the six-fermion process after the PT rearrangement. Solid lines without orientation represent bosons. All loop expressions are now GI, and the gauge dependence enters only through the tree propagators of the gauge bosons and their respective scalars. The mirror image and crossed graphs of the monodromic graphs are not shown.

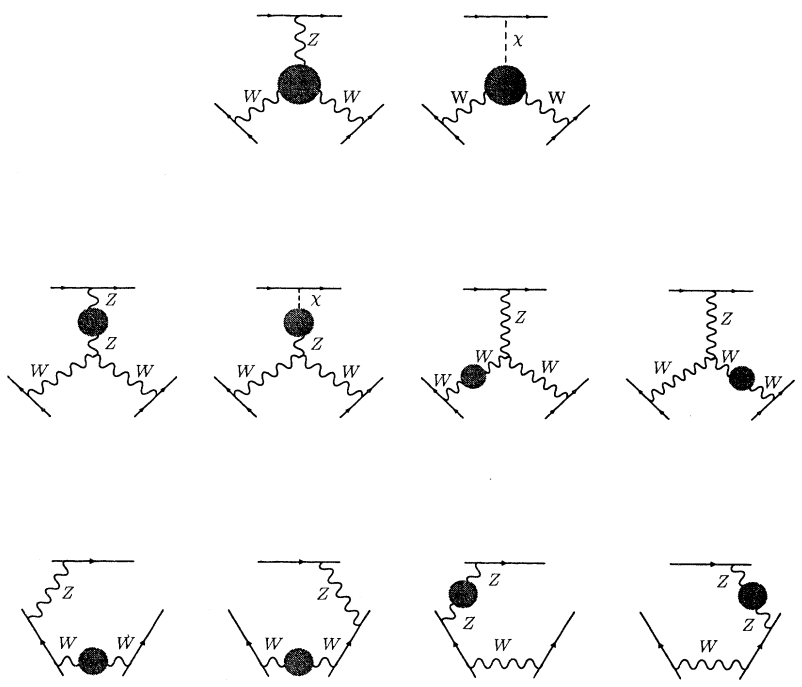

FIG. 9. Graphs contributing a gauge-dependent part of the form $\Delta(q,\xi_Z)$ to the ZWW part of the amplitude.

$$H^{\nu\rho\sigma} = q^{\nu}[U_W^{\alpha\rho}(1)\hat{\Pi}_{\alpha\beta}^W(1)U_W^{\beta\sigma}(1) - U_W^{\alpha\rho}(2)\hat{\Pi}_{\alpha\beta}^W(2)U_W^{\beta\sigma}(2)] + q^{\alpha}\hat{\Pi}_{\alpha\beta}^Z(q)U_Z^{\beta\nu}(q)[U_W^{\sigma\rho}(1) - U_W^{\sigma\rho}(2)], \tag{5.15}$$

where 1,2 in the arguments means p_1 and p_2, respectively.

Since the gauge independence of the amplitude requires that the sum $C_v + C_{se} + C_m^P$ in Eq. (5.11) must vanish, we arrive at the following WI's, relating the ZWW and χWW vertices

$$q^{\mu}\hat{\Gamma}_{\mu\alpha\beta}^{ZW^-W^+} + iM_Z\hat{\Gamma}_{\alpha\beta}^{\chi W^-W^+} = gc[\hat{\Pi}_{\alpha\beta}^W(1) - \hat{\Pi}_{\alpha\beta}^W(2)]. \tag{5.16}$$

Repeating similar steps and requiring the cancellation of the $\Delta_\phi(1)$ and $\Delta_\phi(2)$ gauge dependences, we obtain the following Ward identities, respectively:

$$p_1^{\alpha}\hat{\Gamma}_{\mu\alpha\beta}^{ZW^-W^+} + iM_W\hat{\Gamma}_{\mu\beta}^{Z\phi^-W^+} = gc\left[\hat{\Pi}_{\mu\beta}^W(2) - \hat{\Pi}_{\mu\beta}^Z(q) - \frac{s}{c}\hat{\Pi}_{\mu\beta}^{Z\gamma}(q)\right], \tag{5.17}$$

$$p_2^{\beta}\hat{\Gamma}_{\mu\alpha\beta}^{ZW^-W^+} + iM_W\hat{\Gamma}_{\mu\alpha}^{ZW^-\phi^+} = gc\left[\hat{\Pi}_{\mu\alpha}^Z(q) + \frac{s}{c}\hat{\Pi}_{\mu\alpha}^{Z\gamma}(q) - \hat{\Pi}_{\mu\alpha}^W(1)\right]. \tag{5.18}$$

The WI's for the $\hat{\Gamma}^{\gamma W^-W^+}$ vertex can be derived in a similar manner. We have

$$p_1^{\alpha}\hat{\Gamma}_{\mu\alpha\beta}^{\gamma W^-W^+} + iM_W\hat{\Gamma}_{\mu\beta}^{\gamma\phi^-W^+} = gs\left[\hat{\Pi}_{\mu\beta}^W(2) - \hat{\Pi}_{\mu\beta}^{\gamma}(q) - \frac{c}{s}\hat{\Pi}_{\mu\beta}^{\gamma Z}(q)\right], \tag{5.19}$$

$$p_2^{\beta}\hat{\Gamma}_{\mu\alpha\beta}^{\gamma W^-W^+} + iM_W\hat{\Gamma}_{\mu\alpha}^{ZW^-\phi^+} = gs\left[\hat{\Pi}_{\mu\alpha}^{\gamma}(q) + \frac{c}{s}\hat{\Pi}_{\mu\alpha}^{\gamma Z}(q) - \hat{\Pi}_{\mu\alpha}^W(1)\right], \tag{5.20}$$

which are the counterparts of Eqs. (5.17) and (5.18). It is elementary to derive additional WI's, through straightforward algebraic manipulations of the WI's listed above. For example, the WI

$$iM_Zp_1^{\alpha}\hat{\Gamma}_{\alpha\beta}^{\chi W^-W^+} - iM_Wq^{\alpha}\hat{\Gamma}_{\alpha\beta}^{Z\phi^-W^+} = gc[p_1^{\alpha}\hat{\Pi}_{\alpha\beta}^W(1) + p_2^{\alpha}\hat{\Pi}_{\alpha\beta}^W(2) + q^{\alpha}\hat{\Pi}_{\alpha\beta}^Z(q)] \tag{5.21}$$

or, equivalently,

$$p_1^{\alpha}\hat{\Gamma}_{\alpha\beta}^{\chi W^-W^+} - cq^{\alpha}\hat{\Gamma}_{\alpha\beta}^{Z\phi^-W^+} = gc[c\hat{\Pi}_{\beta}^+(1) + c\hat{\Pi}_{\alpha\beta}^+(2) + \hat{\Pi}_{\beta}^{Z\chi}(q)] \tag{5.22}$$

can be immediately obtained from Eqs. (5.16) and (5.17) after contracting them with the appropriate four-momenta and using the WI's of the self-energies and the fact that $\hat{\Pi}^{Z\gamma}_{\alpha\beta}(q)$ is transverse.

Finally, WI's where the GI TBV's are contracted with two- or three-momenta can be easily derived by demanding the cancellation of gauge dependences stemming from terms with more than one Goldstone boson propagator.

It is interesting to note that an equation analogous to Eq. (5.16) for the $\hat{\Gamma}^{\gamma W^- W^+}$ vertex cannot be derived via this procedure. The reason is simply that all residual dependence on ξ_γ automatically disappears from the final expressions as a result of current conservation, e.g., $q^\mu J^\gamma_\mu = 0$. In order to derive the remaining WI, one must choose a gauge-fixing procedure such as the axial or light-cone gauge, where the dependence of the gauge-boson legs on the gauge parameter does not vanish as a result of current conservation. In fact, this was the way the PT was originally implemented by Cornwall when constructing the one-loop GI gluon self-energy [2]. In the axial (light-cone) gauge, for example, the tree-level propagator for the photon reads

$$\Delta^{\mu\nu}_\gamma(q,n) = \frac{1}{q^2}\left[g_{\mu\nu} - \frac{n_\mu q_\nu + n_\nu q_\mu}{n\cdot q}\right], \tag{5.23}$$

where n_μ is the gauge-fixing parameter (in the light-cone gauge $n_\mu n^\mu = 0$). So after using current conservation, the n with the appropriate Lorentz index will vanish, but the other n will survive and will only vanish if the desired WI's are satisfied. Finally, we obtain

$$\begin{aligned} &q^\mu \hat{\Pi}^{\gamma\gamma}_{\mu\nu}(q) = 0, \\ &q^\mu \hat{\Pi}^{\gamma Z}_{\mu\nu}(q) = 0, \\ &q^\mu \hat{\Pi}^{\gamma\chi}_{\mu}(q) = 0 \Rightarrow \hat{\Pi}^{\gamma\chi}_{\mu}(q) = 0, \end{aligned} \tag{5.24}$$

and

$$q^\mu \hat{\Gamma}^{\gamma W^- W^+}_{\mu\alpha\beta} = gs[\hat{\Pi}^W_{\alpha\beta}(1) - \hat{\Pi}^W_{\alpha\beta}(2)], \tag{5.25}$$

which was first proved in [23] by an explicit one-loop calculation. Clearly, similar WI's can be derived for the gluon self-energy and three-gluon vertex in QCD.

All previous WI's are the one-loop generalizations of the respective *tree-level* WI's. As shown in this section, their validity is crucial for the gauge independence of the S matrix. It is important to emphasize that these WI's make no reference to ghost terms, unlike the corresponding Slavnov-Taylor identities satisfied by the conventional, gauge-dependent vertices.

The WI's derived in this section are also true in the context of the BFM. In fact, in the BFM framework they are true to all orders in perturbation theory; their validity is enforced by the requirement that the Lagrangian be invariant under gauge transformations of the *background fields.* It should be emphasized, however, that the Green's functions of the background fields, which satisfy the aforementioned WI's, display in general a residual dependence on the parameter ξ_Q used to gauge fix the quantum gauge fields. As shown in [27], this remaining gauge dependence can be eliminated by the straightforward application of the PT in the context of the BFM. The analysis presented in this section indicates that these "naive" WI's are not an exclusive property of the BFM, but can be recovered for any type of gauge-fixing procedure via the PT algorithm. Strictly speaking, the WI's we have presented are valid to one-loop order. This is so because our derivation relies on the ability to construct the ξ-independent Green's functions (shown as blobs in Fig. 8) with the PT algorithm, which has only been tested at one loop. If one assumes that this procedure of isolating ξ-independent blobs can be generalized to higher orders in perturbation theory, the generalization of the WI's to higher orders will be relatively straightforward. Even though such an assumption is rather plausible, no such proof exists.

VI. PROOF OF THE WARD IDENTITIES

A. Feynman gauge

In this section we prove by an explicit calculation the first of the Ward identities derived in the previous section, namely, $q^\mu \hat{\Gamma}^{ZW^- W^+}_{\mu\alpha\beta} + iM_Z \hat{\Gamma}^{\chi W^- W^+}_{\alpha\beta} = gc[\hat{\Pi}^W_{\alpha\beta}(1) - \hat{\Pi}^W_{\alpha\beta}(2)]$. We work in the Feynman gauge, where $\xi_i = 1$ for $i = \gamma, W, Z$. To that end, it is more economical to act with q^μ directly on the individual graphs of $\hat{\Gamma}^Z_{\mu\alpha\beta}$ and try to generate the RHS of Eq. (5.16). The Feynman diagrams contributing to the GI W self-energies of the RHS are shown in Fig. 10. The closed expression for the GI W self-energy has been obtained in [16], and it is

$$\hat{\Pi}^W_{\alpha\beta}(q) = \Pi^W_{\alpha\beta}(q)|_{\xi=1} + 4U^{-1}_{\alpha\beta}(q)[s^2 I_{W\gamma}(q) + c^2 I_{WZ}(q)]. \tag{6.1}$$

We also emphasize that all necessary cancellations between graphs or parts of graphs are evident before any of the loop momentum integrations are carried out.

To begin with, we note that all pinch parts originating from the top (neutral current) fermion line automatically cancel on the LHS of Eq. (5.16) by virtue of the second and third equations of Eqs. (3.13).

We start by considering the fermion graphs Fig. 5, diagram (1), and Fig. 6, diagram (1). This subset of graphs is automatically GI and receives therefore no pinch contributions. After a straightforward calculation we obtain (in what follows we have pulled out a common factor of gc from the RHS of all equations)

$$q^\mu V^1_{\mu\alpha\beta} + iM_Z \mathcal{S}^1_{\alpha\beta} = \Pi^1_{\alpha\beta}(1) - \Pi^1_{\alpha\beta}(2), \tag{6.2}$$

where $\Pi^1_{\alpha\beta}$ corresponds to the self-energy diagram (1) of Fig. 10.

The remaining diagrams can be divided into three classes depending on the type of internal boson propagators they contain. Following the notation of Eq. (4.3), these classes are denoted as (i) WWV diagrams, where $V = \gamma, Z$ [Fig. 5, diagrams (2)–(22), Fig. 6, diagrams (2)–(13)], (ii) WWH diagrams [Fig. 5, diagrams (23)–(28), Fig. 6, diagrams (14), (15)], and (iii) ZHW diagrams [Fig. 5, diagrams (29)–(34), Fig. 6, diagrams (16)–(21)].

WWV graphs: Vector boson graphs

$$\sum_{i=2}^{8} q^\mu V^i_{\mu\alpha\beta} = \sum_{i=2}^{3}[\Pi^i_{\alpha\beta}(1) - \Pi^i_{\alpha\beta}(2)] - \sum_{V=\gamma Z} g_V^2 \Delta M^2_{WV} \int (WWV) q^\rho \Gamma_{\rho\alpha\beta}(q, p_1 - k, p_2 + k)$$
$$+ \sum_{V=\gamma Z} g_V^2 \int W(k+p_1) V(k) k_\alpha q_\beta + (1 \leftrightarrow 2)$$
$$- \sum_{V=\gamma Z} g_V^2 \int (WWV) q \cdot (k - p_2) k_\alpha (k - p_2)_\beta + (1 \leftrightarrow 2)$$
$$-2g^2[U_W^{-1}(1)_{\alpha\beta} - U_W^{-1}(2)_{\alpha\beta}] \int W(k+p_1) W(k - p_2)$$
$$-U_W^{-1}(1)_{\alpha\rho} \sum_{V=\gamma Z} g_V^2 \int (WWV)[q^\rho k_\beta + q^\lambda \Gamma_{\lambda\rho\beta}(k - p_2, -k, p_2)] + (1 \leftrightarrow 2), \tag{6.3}$$

where the tree-level WI's of Eq. (5.10), as well as the identities given in Eqs. (4.11) and (4.12) of [23], have been used. The notation $(1 \leftrightarrow 2)$ means to interchange in the preceeding term $p_1 \leftrightarrow -p_2$ and $\alpha \leftrightarrow \beta$. From the terms appearing on the RHS of Eq. (6.3), only the first is part of the RHS of the WI's we attempt to prove. All other terms will cancel against other contributions from the remaining graphs. In particular, the leftover term of the second line will cancel against similar terms coming from the graphs which contain unphysical Goldstone bosons. Similarly, the terms in the next two lines of Eq. (6.3) will cancel against corresponding leftovers from the ghost graphs. Finally, the last two lines of Eq. (6.3), which display the characteristic pinch structure, will cancel against some of the pinch contributions to the ZWW vertex. All these cancellations will become evident in what follows.

We next consider the ghost graphs [Fig. 5, diagrams (9)–(12), and Fig. 6, diagrams (2)–(5)]. We have

$$\sum_{i=9}^{12} q^\mu V^i_{\mu\alpha\beta} = \sum_{i=4}^{7}[\Pi^i_{\alpha\beta}(1) - \Pi^i_{\alpha\beta}(2)] - \sum_{V=\gamma Z} g_V^2 \int W(k+p_1) V(k) k_\alpha q_\beta + (1 \leftrightarrow 2)$$
$$+ \sum_{V=\gamma Z} g_V^2 \int (WWV) q \cdot (k - p_2) k_\alpha (k - p_2)_\beta + (1 \leftrightarrow 2) \tag{6.4}$$

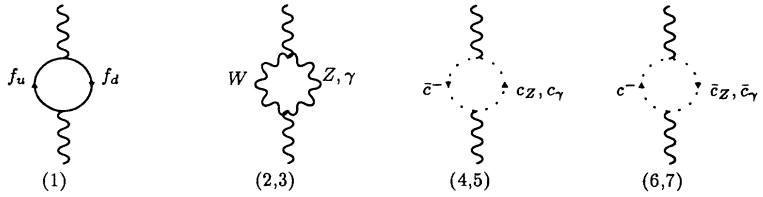

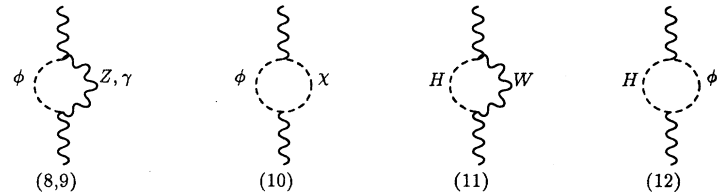

FIG. 10. Feynman diagrams contributing to the W self-energy. Graph (13) is particular to the BFM.

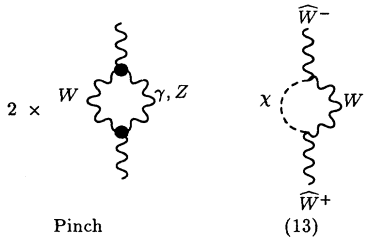

and

$$iM_Z\sum_{i=2}^{5}\mathcal{S}^i_{\alpha\beta}=-\frac{M_W^2}{2c^2}\sum_{V=\gamma Z}g_V^2\int(WWV)(k_\alpha p_{2\beta}+k_\beta p_{1\alpha}). \tag{6.5}$$

We see that the leftover terms of Eq. (6.4) cancel against parts of Eq. (6.3) as expected. The contribution of Eq. (6.5) will cancel against pinch contributions to the χWW vertex. Similarly, the graphs containing unphysical Goldstone bosons [Fig. 5, diagrams (13)–(22), and Fig. 6, diagrams (6)–(13)] yield

$$\sum_{i=13}^{16}q^\mu V^i_{\mu\alpha\beta}+iM_Z\sum_{i=6}^{9}\mathcal{S}^i_{\alpha\beta}=g^2s^2M_W^2\sum_{V=\gamma,Z}b_V\int(WWV)q^\rho\Gamma_{\rho\alpha\beta}(q,p_1-k,p_2+k)$$
$$+g^2M_W^2\frac{s^2}{2c^2}[U_W^{-1}(1)_{\alpha\beta}-U_W^{-1}(2)_{\alpha\beta}]\sum_{V=\gamma,Z}b_VJ_{WWV}, \tag{6.6}$$

$$\sum_{i=17}^{18}q^\mu V^i_{\mu\alpha\beta}+iM_Z\sum_{10}^{13}\mathcal{S}^i_{\alpha\beta}=\sum_{i=8}^{9}[\Pi^i_{\alpha\beta}(1)-\Pi^i_{\alpha\beta}(2)], \tag{6.7}$$

$$\sum_{i=19}^{21}q^\mu V^i_{\mu\alpha\beta}=\Pi^{10}_{\alpha\beta}(1)-\Pi^{10}_{\alpha\beta}(2)-\frac{g^2}{8c^2}\int W(k)[Z(k+p_1)-Z(k-p_2)](2k+p_1)_\alpha(2k-p_2)_\beta, \tag{6.8}$$

$$q^\mu V^{22}_{\mu\alpha\beta}=0. \tag{6.9}$$

The first term on the RHS of Eq. (6.6) cancels the appropriate term in Eq. (6.3) after employing the elementary identity $-gcg_V^2\Delta M^2_{WV}=-b_Vg^3cs^2M_W^2$, where $b_\gamma=+1$ and $b_Z=-1$. The second term on the RHS of Eq. (6.6) will cancel against pinch contributions to the χWW vertex. Finally, we note that the leftover term on the RHS of Eq. (6.8) contains only two internal propagators.

The pinch parts give

$$q^\mu[B^-_{\mu\rho\beta}U_W^{-1}(p_1)^\rho_\alpha+B^+_{\mu\alpha\rho}U_W^{-1}(p_2)^\rho_\beta]=2[U_W^{-1}(p_1)_{\alpha\beta}+U_W^{-1}(p_2)_{\alpha\beta}]\sum_{V=\gamma,Z}g_V^2[I_{WV}(p_1)-I_{WV}(p_2)] \tag{6.10}$$
$$+U_W^{-1}(p_2)_{\beta\rho}\sum_{V=\gamma,Z}g_V^2\int(WWV)[q^\rho k_\alpha+q^\lambda\Gamma_{\lambda\alpha\rho}(-k-p_1,p_1,k)]+(1\leftrightarrow2)\ ,$$

$$-2g^2q^\mu\Gamma_{\mu\alpha\beta}[\cdots]=2g^2[U_W^{-1}(p_1)_{\alpha\beta}-U_W^{-1}(p_2)_{\alpha\beta}][\cdots], \tag{6.11}$$

where the ellipses in the square brackets in Eq. (6.11) represent the terms of the second line of Eq. (4.34) multiplying $\Gamma_{\mu\alpha\beta}$:

$$\sum_{i=1}^{4}q^\mu(R^i_{\mu\alpha\beta}+L^i_{\mu\alpha\beta})-g^2M_W^2[p_{2\beta}q_\alpha-p_{1\alpha}q_\beta]\left[\frac{s^2}{c^2}J_{WW\gamma}+\frac{1-2s^2}{2c^2}J_{WWZ}\right], \tag{6.12}$$

$$iM_Z\sum_{i=1}^{2}(\mathcal{R}^i_{\alpha\beta}+\mathcal{L}^i_{\alpha\beta})=g^2M_W^2\frac{s^2}{2c^2}[U^{-1}_{\alpha\beta}(p_1)-U^{-1}_{\alpha\beta}(p_2)]\sum_{V=\gamma Z}b_VJ_{WWV}, \tag{6.13}$$

$$iM_Z(\mathcal{R}^3_{\alpha\beta}+\mathcal{L}^3_{\alpha\beta})=g^2M_W^2\frac{s^2}{2c^2}\int(WW\gamma)[(k-2q)_\alpha p_{2\beta}+p_{1\alpha}(k+2q)_\beta], \tag{6.14}$$

$$iM_Z\sum_{i=4}^{5}(\mathcal{R}^i_{\alpha\beta}+\mathcal{L}^i_{\alpha\beta})=+g^2\frac{M_W^2}{2}\int(WWZ)[k_\alpha p_{2\beta}+p_{1\alpha}k_\beta]-g^2M_W^2\frac{1-2s^2}{2c^2}[p_{2\beta}q_\alpha-p_{1\alpha}q_\beta]J_{WWZ}. \tag{6.15}$$

At this point we note that the contributions of the pinch parts cancel all the remaining leftovers of all other graphs we have considered thus far, except for the leftover term of Eq. (6.8). If we now collect all W self-energy terms on the RHS, we note that all pinch and regular graphs have already appeared, except for the two graphs containing an internal Higgs boson, shown in Fig. 10, diagrams (11) and (12).

Next, we consider the WWH graphs

$$\sum_{i=23}^{25} q^\mu V^i_{\mu\alpha\beta} + iM_Z \sum_{i=14}^{15} \mathcal{S}^i_{\alpha\beta} = \Pi^{11}_{\alpha\beta}(1) - \Pi^{11}_{\alpha\beta}(2) - \frac{g^2 M_W^2}{4c^2}\int (WWH)[k_\alpha p_{2\beta} + k_\beta p_{1\alpha}] - \frac{g^2 M_W^2}{2}[p_{1\alpha}p_{1\beta} - p_{2\alpha}p_{2\beta}]J_{WWH}, \tag{6.16}$$

$$\sum_{i=26}^{28} q^\mu V^i_{\mu\alpha\beta} = \Pi^{12}_{\alpha\beta}(1) - \Pi^{12}_{\alpha\beta}(2) - \frac{g^2}{8c^2}\int W(k)[H(k+p_1) - H(k-p_2)](2k+p_1)_\alpha (2k-p_2)_\beta. \tag{6.17}$$

The relevant pinch diagrams of this class contributing to the ZWW vertex give

$$q^\mu(R^5_{\mu\alpha\beta} + L^5_{\mu\alpha\beta}) = \frac{g^2 M_W^2}{2}[p_{1\alpha}p_{1\beta} - p_{2\alpha}p_{2\beta}]J_{WWH}, \tag{6.18}$$

whereas the ones contributing to the χWW vertex give

$$iM_Z(\mathcal{R}^6_{\alpha\beta} + \mathcal{L}^6_{\alpha\beta}) = \frac{g^2 M_W^2}{4c^2}\int (WWH)[k_\alpha p_{2\beta} + k_\beta p_{1\alpha}]. \tag{6.19}$$

It is now evident that all the W self-energy terms which constitute the RHS of the WI's have already appeared. The only two redundant terms are (i) the leftover term of Eq. (6.8) and (ii) the leftover term of Eq. (6.18), which survives after Eqs. (6.16)–(6.19) have been added by parts. Like the term in (i) it also contains two internal propagators. Both terms will cancel exactly against the entire contribution of the graphs belonging to the ZHW class, which we now proceed to evaluate.

We will only evaluate the diagrams where the Higgs boson appears on the left. The mirror graphs, with the Higgs boson on the right, can be treated in an exactly analogous way:

$$q^\mu V^{30}_{\mu\alpha\beta} = -\frac{g^2 M_W^2}{c^2}\int (HZW) q^\mu \Gamma_{\mu\alpha\beta}(-k-p_1, p_1, k), \tag{6.20}$$

$$iM_Z \mathcal{S}^{17}_{\alpha\beta} = \frac{g^2 M_W^2}{c^2}\int (HZW) q^\mu \Gamma_{\mu\alpha\beta}(-k-p_1, p_1, k) - g^2\frac{M_W^2}{2c^2}U_W^{-1}(p_2)_{\alpha\beta}J_{HZW} - g^2\frac{M_W^2}{2c^2}\int (HZW)k_\alpha k_\beta + g^2\frac{M_W^2}{2c^2}g_{\alpha\beta}I_{HZ}(q). \tag{6.21}$$

The last term on the RHS of the last equation will cancel against an equal and opposite contribution coming from the mirror diagram $S^{18}_{\alpha\beta}$:

$$q^\mu V^{32}_{\mu\alpha\beta} = -\frac{g^2 M_Z^2 s^2}{2c^2}q_\beta \int (HZW)(2k+p_1)_\alpha\ , \tag{6.22}$$

$$iM_Z \mathcal{S}^{19}_{\alpha\beta} = \frac{g^2 M_Z^2 s^2}{2c^2}q_\beta \int (HZW)(2k+p_1)_\alpha - g^2\frac{M_Z^2 s^2}{4c^2}\int (HZW)(2k+p_1)_\alpha (k-p_2)_\beta, \tag{6.23}$$

$$q^\mu V^{34}_{\mu\alpha\beta} = \frac{g^2}{8c^2}(M_Z^2 - M_H^2)\int (HZW)(2k+p_1)_\alpha (2k-p_2)_\beta + \frac{g^2}{8c^2}\int W(k)[H(k+p_1) - Z(k-p_2)](2k+p_1)_\alpha (2k-p_2)_\beta, \tag{6.24}$$

$$iM_Z \mathcal{S}^{21}_{\alpha\beta} = \frac{g^2}{8c^2}M_H^2 \int (HZW)(2k+p_1)_\alpha (2k-p_2)_\beta. \tag{6.25}$$

The pinch parts are

$$q^\mu L^6_{\mu\alpha\beta} + iM_Z \mathcal{L}^7_{\alpha\beta} = -g^2 \frac{M_W^2}{2c^2} p_{1\alpha} \int (HZW) k_\beta, \tag{6.26}$$

$$iM_Z(\mathcal{R}^8_{\alpha\beta} + \mathcal{R}^{8\mathrm{cr}}_{\alpha\beta}) = g^2 \frac{M_W^2}{2c^2} U_W^{-1}(p_2)_{\alpha\beta} J_{HZW} \ , \tag{6.27}$$

$$iM_Z(\mathcal{R}^9_{\alpha\beta} + \mathcal{R}^{9\mathrm{cr}}_{\alpha\beta}) = g^2 \frac{M_Z^2(1-2s^2)}{8c^2} p_{2\beta} \int (HZW)(2k+p_1)_\alpha. \tag{6.28}$$

When all the above equations, together with the corresponding contributions from the mirror graphs, are added by parts, all terms on the RHS cancel among each other as expected, except for the terms with two internal propagators, from Eq. (6.24) and the mirror graph result, which exactly cancel the leftover terms mentioned previously, (i) and (ii). This concludes the proof of the WI of Eq. (5.16), which is a central result of this paper. It is obvious from the previous proof that the pinch parts are instrumental for the validity of Eq. (5.16).

B. Unitary gauge

The fact that the WI's of Green's functions constructed via the PT hold regardless of the gauge in which one chooses to work can be most effectively demonstrated by proving their validity in different gauges. Although the usual graphs of a Green's function as well as its pinch parts assume different forms in different gauges, when summed they nevertheless combine into a unique expression independent of any specific gauge. In this section we will work in the unitary gauge, where additional pinch parts can originate from the longitudinal parts of the gauge-boson propagators.

We note that, even though the unitary gauge has been traditionally considered pathological, in the sense that it gives rise to nonrenormalizable Green's functions, in the context of the PT it can be treated on an equal footing as the renormalizable R_ξ gauges. In particular, as shown in [29] the application of the PT in the context of the unitary gauge gives rise to *renormalizable* Green's functions which are in fact identical to the ξ-independent Green's functions obtained in the framework of the R_ξ gauges.

Applying the PT to the case of the three-boson vertices in the unitary gauge, we have verified that the WI's of Eqs. (5.16) and (5.25) again hold true. We point out that although the usual vertex graphs are fewer in this gauge the graphs which can contribute pinch parts are quite numerous, a fact that makes calculations lengthier. We therefore do not present the entire proof of the WI's, but only outline the steps in its derivation.

The usual $\gamma W^- W^+$ vertex diagrams in this gauge are shown in Fig. 5, diagrams (1)–(8) and (23), while for the ZW^-W^+ vertex we have the additional graphs (29) and (30) of the same figure. The relevant W self energy diagrams in the unitary gauge are those shown in Fig. 10, diagrams (1)–(3) and (11). The vertex graphs will be denoted as $\mathcal{V}^i_{\mu\alpha\beta}$ and the self-energy graphs as $\mathcal{U}^i_{\alpha\beta}$, where the index i counts the corresponding graphs of Figs. 5 and 10.

The interesting feature of the unitary gauge is that the WI of the $\gamma W^- W^+$ vertex is satisfied *separately* by the usual and pinch parts, as one can verify immediately.

For the fermion graphs, Eq. (6.2) holds as usual since they are gauge invariant, e.g., $V^1_{\mu\alpha\beta} = \mathcal{V}^1_{\mu\alpha\beta}$ and $\Pi^1_{\alpha\beta} = \mathcal{U}^1_{\alpha\beta}$. The boson graphs give

$$q^\mu \mathcal{V}^{2,3}_{\mu\alpha\beta} + q^\mu \mathcal{V}^{6,5}_{\mu\alpha\beta} + q^\mu \mathcal{V}^{8,7}_{\mu\alpha\beta} = gc[\mathcal{U}^{2,3}_{\alpha\beta}(1) - \mathcal{U}^{2,3}_{\alpha\beta}(2)] \tag{6.29}$$

and

$$q^\mu \mathcal{V}^4_{\mu\alpha\beta} = 0. \tag{6.30}$$

From the Higgs diagram we get

$$q^\mu \mathcal{V}^{23}_{\mu\alpha\beta} = gc[\mathcal{U}^{11}_{\alpha\beta}(1) - \mathcal{U}^{11}_{\alpha\beta}(2)]. \tag{6.31}$$

For the γWW vertex the above equations when summed give

$$q^\mu \mathcal{V}^\gamma_{\mu\alpha\beta} = gc[\mathcal{U}^W_{\alpha\beta}(1) - \mathcal{U}^W_{\alpha\beta}(2)]. \tag{6.32}$$

Evidently, the Ward identity holds already for the usual vertex graphs *before* any pinch contributions are included. One can then verify that the vertexlike pinch contributions in the unitary gauge $(\mathcal{V}^\gamma_{\mu\alpha\beta})^P$ (some of the additional ones, specific to the unitary gauge, are shown in Fig. 11), when contracted with q^μ, yield

$$g^\mu (\mathcal{V}^\gamma_{\mu\alpha\beta})^P = gc[\mathcal{P}^W_{\alpha\beta}(1) - \mathcal{P}^W_{\alpha\beta}(2)], \tag{6.33}$$

where $\mathcal{P}^W_{\alpha\beta}$ are the relevant propagatorlike parts to be appended to the W self-energy in the unitary gauge. As shown in [29], the W self-energy obtained via the PT in the unitary gauge is identical to the one obtained via the PT in the context of the R_ξ gauges: namely,

$$\hat{\Pi}^W_{\alpha\beta}(q) = \mathcal{U}^W_{\alpha\beta} + \mathcal{P}^W_{\alpha\beta}. \tag{6.34}$$

Adding Eqs. (6.4) and (6.5) by parts, we arrive again at the WI of Eq. (5.25).

For the ZWW vertex the proof proceeds in an analogous way. For the class of graphs that are common to both vertices γWW and ZWW, the proof is identical. The WI is again satisfied *separately* by the regular vertex and pinch graphs. There are, however, two additional classes of contributions that need be considered. First, there are the extra regular vertex graphs (29) and (30) of Fig. 5 along with similar box graphs that will contribute a pinch part to the vertex; all the above graphs contain a Higgs particle. Second, unlike the photon case, the vertexlike pinch parts originating from boxed where the pinching takes place at the leg of the Z (fermion line on the top) do not vanish when contracted with q^μ. Since all propagator graphs of the W have already appeared on the left-hand side of the WI's, the sole role of these graphs is to provide a leftover expression which is recognized as being equal to $\hat{\Gamma}^{\chi W^- W^+}_{\alpha\beta}$. Of course, in the context of the unitary gauge this expression cannot be identified with a χWW vertex, because there are no χ fields to begin with.

C. Feynman background field gauge

In this section we prove the validity of the WI's of Eqs. (5.16) and (5.25) in the Feynman gauge of the BFM.

In the BFM every bosonic field is decomposed into two parts, the quantum field Φ and the background field $\hat{\Phi}$, e.g., $\Phi \to \Phi + \hat{\Phi}$. In the path integral one integrates the quantum fields only, whereas the background fields are treated as additional sources; consequently, only the quantum fields appear inside loops.

The ordinary gauge transformation of the gauge fields, for example, W^a_μ, $a = 1,2,3$, and B_μ in the case of an SU(2)×U(1) group, is also split into two transformations. One of them corresponds to an ordinary gauge transformation, but only for the background fields $\hat{W}^a_\mu, \hat{B}_\mu$, and is therefore called a background gauge transformation. By judiciously adding an unconventional gauge-fixing term for the quantum fields, we can promote this transformation to a symmetry of the Lagrangian. Therefore the Green's functions of the background fields are guaranteed to be background gauge invariant, namely, $\Gamma(\hat{W}^a_\mu \hat{B}_\nu \ldots) = \Gamma(\hat{W}'^a_\mu \hat{B}'_\nu \ldots)$. As a result of this invariance, the naive WI's of Sec. V are satisfied. Note, however, that these Green's functions depend in general on the gauge parameters ξ_W, ξ_B used to gauge fix the quantum fields W^a_μ and B_μ which appear inside their loops. In this formulation, S matrix elements are calculated by forming trees of background Green's functions connected to each other by tree-level background field propagators; at this point, the background fields also require gauge fixing.

This gauge fixing is completely independent from the gauge fixing of the quantum fields, and the parameters $\hat{\xi}_W, \hat{\xi}_B$ may be in general different from the parameters ξ_W, ξ_B.

We choose to work in the Feynman gauge of the BFM where $\xi_W = \xi_B \equiv \xi_Q = 1$. As was shown in [25,27], at the one-loop level this particular gauge choice gives rise to background Green's functions which are identical to the GI Green's functions constructed via the PT. No formal understanding of this correspondence has yet been established; the aforementioned agreement has been verified by comparing all Green's functions constructed so far at one loop via the PT with the corresponding BFM Green's functions. The operational reason for this identity of results is that pinching turns out to be zero in this particular gauge. To this end we remind the reader that pinch parts can originate in three ways: (i) from the longitudinal part of gauge-boson propagators, (ii) from three gauge-boson vertices, and (iii) from vertices with two Goldstone bosons and one gauge boson.

All these can provide the appropriate momenta which when contracted with a γ matrix will cancel a fermion propagator. By simple inspection of the Feynman rules of this gauge, one immediately recognizes that all the necessary pieces that could generate pinch terms are missing. First of all, since this is a Feynman type of gauge, there are no longitudinal parts for the gauge-boson propagators. Second, one observes that in this gauge the three-gauge-boson vertex between a background and two quantum gauge fields (which is gauge dependent even at tree level) assumes the form

$$\Gamma_{\alpha\beta\gamma}(q,k,-q-k) = \Gamma^F_{\alpha\beta\gamma} + \left(1 - \frac{1}{\xi_Q}\right)\Gamma^P_{\alpha\beta\gamma}, \quad (6.35)$$

where

$$\Gamma^F_{\alpha\beta\gamma} = (2k+q)_\alpha g_{\beta\gamma} - 2q_\beta q_{\gamma\alpha} + 2q_\gamma g_{\alpha\beta} \quad (6.36)$$

and

$$\Gamma^P_{\alpha\beta\gamma} = -k_\beta g_{\gamma\alpha} - (k+q)_\gamma g_{\alpha\beta}. \quad (6.37)$$

We see immediately that by setting $\xi_Q = 1$ the $\Gamma^P_{\alpha\beta\gamma}$ part, which is the only one that can pinch, disappears. Finally, the elementary vertices of the form $\hat{\phi}\phi G$, where $\hat{\phi}, \phi$ are scalars (Higgs or unphysical bosons would be Goldstone bosons) and G_μ a quantum gauge field (W^a_μ, B_μ), depend only on the momentum carried by the background field $\hat{\phi}$: namely,

$$\Gamma^{\hat{\phi}\phi G}_\mu(q,k,-q-k) \propto q_\mu. \quad (6.38)$$

Therefore they also cannot trigger pinching. Consequently, since pinching has been rendered trivial (zero) in this gauge, one readily concludes that the Green's functions constructed via the PT in any gauge will be identical to the conventional Green's functions of the Feynman gauge of the BFM, i.e.,

$$\hat{\Pi}^W_{\alpha\beta} = \Pi^{\hat{W}}_{\alpha\beta}, \quad \hat{\Gamma}^{ZW^-W^+}_{\mu\alpha\beta} = \Gamma^{\hat{Z}\hat{W}^-\hat{W}^+}, \quad \text{etc.} \quad (6.39)$$

We now proceed to the proof of the WI's of Eqs. (5.16) and (5.25). We need to consider only the usual vertex and self-energy graphs in this gauge. The vertex graphs are those of Figs. 5 and 6 plus the additional ones of Figs. 11 and 12. Note that for the $\chi W^- W^+$ vertex there are no ghost graphs in this gauge; so for this paragraph the graphs of Fig. 6, diagrams (2)–(5), are replaced by those

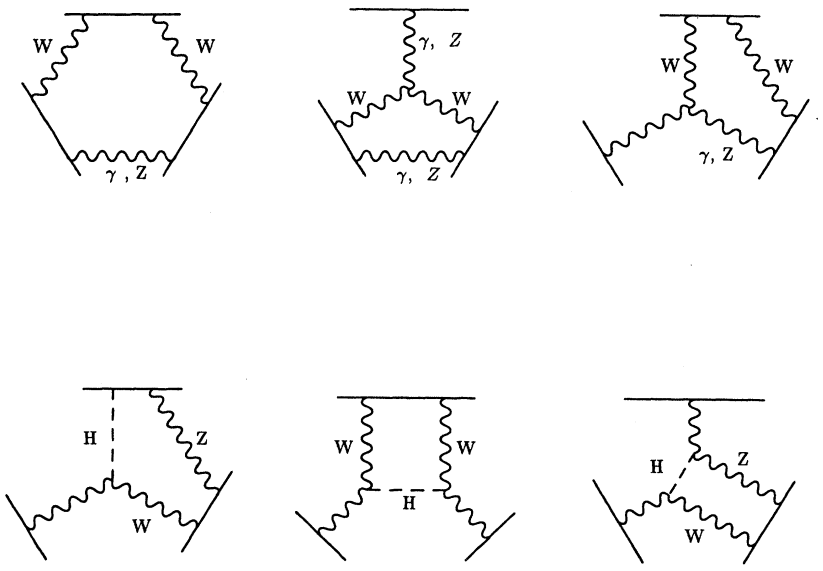

FIG. 11. Box graphs that in the unitary gauge can provide vertexlike pinch parts. In these graphs pinching is triggered through the longitudinal part of the vector bosons' propagators.

of Fig. 13, diagrams (2)–(5). The modifications needed for the W self-energy graphs are that an additional graph [Fig. 10, diagram (13)] must be included and the pinch graph must be removed. In all these figures the external legs are now considered to be background fields.

We will use the same symbols for the various diagrams as in Sec. VI A, even though now, since we work in a different gauge, they correspond in general to different expressions. So $V^i_{\mu\alpha\beta}$ will correspond to a ZW^-W^+ vertex diagram, $S^i_{\alpha\beta}$ to a χW^-W^+ vertex, and $\Pi^i_{\alpha\beta}$ to a W self-energy graph.

By acting with q^μ on the three-gauge-boson vertex graphs, we readily obtain the following results.

For the fermion graphs,

$$q^\mu V^1_{\mu\alpha\beta} + iM_Z S^1_{\alpha\beta} = gc[\Pi^1_{\alpha\beta}(1) - \Pi^1_{\alpha\beta}(2)]. \quad (6.40)$$

For the gauge boson graphs,

$$q^\mu V^{2,3}_{\mu\alpha\beta} + q^\mu V^{4,5}_{\mu\alpha\beta} + q^\mu V^{6,7}_{\mu\alpha\beta} = gc[\Pi^{2,3}_{\alpha\beta}(1) - \Pi^{2,3}_{\alpha\beta}(2)], \quad (6.41)$$

$$g^\mu V^8_{\mu\alpha\beta} = 0. \quad (6.42)$$

For the ghost graphs,

$$q^\mu V^{9,10}_{\mu\alpha\beta} + q^\mu V^{35,36}_{\mu\alpha\beta} + q^\mu V^{37,38}_{\mu\alpha\beta} = gc[\Pi^{5,4}_{\alpha\beta}(1) - \Pi^{4,5}_{\alpha\beta}(2)], \quad (6.43)$$

$$q^\mu V^{39}_{\mu\alpha\beta} = 0, \quad (6.44)$$

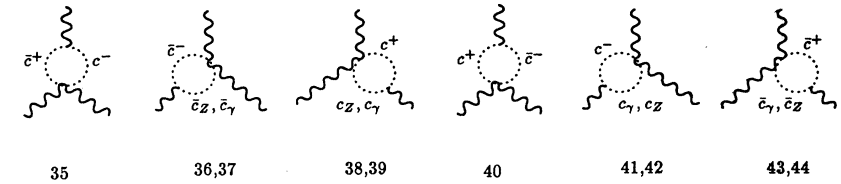

FIG. 12. Additional γWW and ZWW vertex graphs of the Feynman gauge of the background field method. Together with those of Fig. 5, they are denoted by $V^i_{\mu\alpha\beta}$ in Sec. VI C.

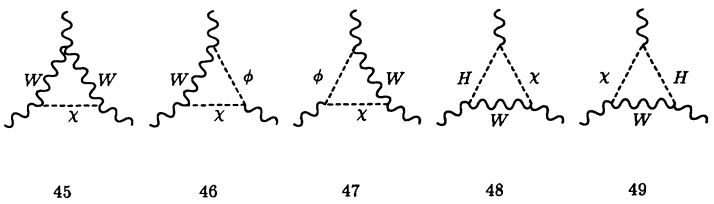

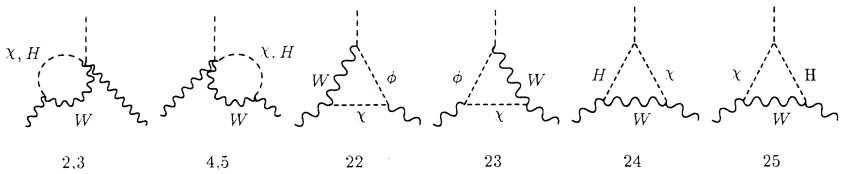

FIG. 13. Additional χWW vertex graphs of the Feynman gauge of the background field method. Together with those of Fig. 5, they are denoted by $S^i_{\mu\alpha\beta}$ in Sec. IV C. Graphs (2)–(5) replace the ghost graphs (2)–(5) of Fig. 6, which do not exist in this gauge.

$$q^\mu V^{11,12}_{\mu\alpha\beta} + q^\mu V^{41,40}_{\mu\alpha\beta} + q^\mu V^{43,42}_{\mu\alpha\beta} = gc[\Pi^{7,6}_{\alpha\beta}(1) - \Pi^{4,5}_{\alpha\beta}(2)], \quad (6.45)$$

$$q^\mu V^{44}_{\mu\alpha\beta} = 0. \quad (6.46)$$

In fact, Eq. (6.43) is identical to Eq. (6.45) part by part, and correspondingly Eq. (6.44) is identical to Eq. (6.46). This is so because ghost graphs in this gauge result in identical expressions regardless of the orientation of the ghost line.

For the Goldstone and gauge boson graphs we obtain the following.

For the WWV propagators,

$$q^\mu V^{13,14}_{\mu\alpha\beta} + iM_Z S^{7,6}_{\alpha\beta} = 0, \quad (6.47)$$

$$q^\mu V^{15,16}_{\mu\alpha\beta} + iM_Z S^{9,8}_{\alpha\beta} = 0, \quad (6.48)$$

$$q^\mu V^{17,18}_{\mu\alpha\beta} + iM_Z S^{11,10}_{\alpha\beta} + iM_Z S^{13,12}_{\alpha\beta} = gc[\Pi^{9,8}_{\alpha\beta}(1) - \Pi^{9,8}_{\alpha\beta}(2)], \quad (6.49)$$

$$q^\mu V^{22}_{\mu\alpha\beta} = 0, \quad (6.50)$$

$$q^\mu V^{45}_{\mu\alpha\beta} = gc[\Pi^{13}_{\alpha\beta}(1) - \Pi^{13}_{\alpha\beta}(2)], \quad (6.51)$$

$$q^\mu V^{46}_{\mu\alpha\beta} + iM_Z S^{22}_{\alpha\beta} = 0, \quad (6.52)$$

$$q^\mu V^{47}_{\mu\alpha\beta} + iM_Z S^{23}_{\alpha\beta} = 0. \quad (6.53)$$

For the WWH propagators,

$$q^\mu V^{23}_{\mu\alpha\beta} = gc[\Pi^{11}_{\alpha\beta}(1) - \Pi^{11}_{\alpha\beta}(2)], \quad (6.54)$$

$$q^\mu V^{24}_{\mu\alpha\beta} + iM_Z S^{14}_{\alpha\beta} = 0, \quad (6.55)$$

$$q^\mu V^{25}_{\mu\alpha\beta} + iM_Z S^{15}_{\alpha\beta} = 0. \quad (6.56)$$

For the HZW and ZHW propagators,

$$q^\mu V^{29}_{\mu\alpha\beta} + iM_Z S^{17}_{\alpha\beta} = 0, \quad (6.57)$$

and the mirror image graph

$$q^\mu V^{30}_{\mu\alpha\beta} + iM_Z S^{16}_{\alpha\beta} = 0, \quad (6.58)$$

$$q^\mu V^{31}_{\mu\alpha\beta} + iM_Z S^{19}_{\alpha\beta} = 0, \quad (6.59)$$

and the mirror image graph

$$q^\mu V^{32}_{\mu\alpha\beta} + iM_Z S^{18}_{\alpha\beta} = 0, \quad (6.60)$$

$$q^\mu V^{49}_{\mu\alpha\beta} + iM_Z S^{25}_{\alpha\beta} + iM_Z S^{3}_{\alpha\beta} + iM_Z S^{4}_{\alpha\beta} = 0, \quad (6.61)$$

$$q^\mu V^{48}_{\mu\alpha\beta} + iM_Z S^{24}_{\alpha\beta} + iM_Z S^{2}_{\alpha\beta} + iM_Z S^{5}_{\alpha\beta} = 0. \quad (6.62)$$

The rest of the Goldstone boson graphs give

$$q^\mu V^{19}_{\mu\alpha\beta} + q^\mu V^{20}_{\mu\alpha\beta} + q^\mu V^{21}_{\mu\alpha\beta} = gc[\Pi^{10}_{\alpha\beta}(1) - \Pi^{10}_{\alpha\beta}(2)] - \frac{g^3}{8c}\int Z(k)W(k+p_1)(2k+p_1)_\alpha(2k+p_1-q)_\beta \quad (6.63)$$

$$+\frac{g^3}{8c}\int Z(k)W(k-p_2)(2k-p_2)_\beta(2k-p_2+q)_\alpha\ , \quad (6.64)$$

$$q^\mu V^{26}_{\mu\alpha\beta} + q^\mu V^{27}_{\mu\alpha\beta} + q^\mu V^{28}_{\mu\alpha\beta} = gc[\Pi^{12}_{\alpha\beta}(1) - \Pi^{12}_{\alpha\beta}(2)] - \frac{g^3}{8c}\int H(k)W(k+p_1)(2k+p_1)_\alpha(2k+p_1-q)_\beta \quad (6.65)$$

$$+\frac{g^3}{8c}\int H(k)W(k-p_2)(2k-p_2)_\beta(2k-p_2+q)_\alpha\ , \quad (6.66)$$

$$q^\mu V^{33}_{\mu\alpha\beta} + iM_Z S^{21}_{\alpha\beta} = \frac{g^3}{8c}\int H(k)W(k+p_1)(2k+p_1)_\alpha(2k+p_1-q)_\beta$$
$$-\frac{g^3}{8c}\int Z(k)W(k-p_2)(2k-p_2)_\beta(2k-p_2+q)_\alpha\ , \tag{6.67}$$

$$q^\mu V^{34}_{\mu\alpha\beta} + iM_Z S^{20}_{\alpha\beta} = \frac{g^3}{8c}\int Z(k)W(k+p_1)(2k+p_1)_\alpha(2k+p_1-q)_\beta$$
$$-\frac{g^3}{8c}\int H(k)W(k-p_2)(2k-p_2)_\beta(2k-p_2+q)_\alpha. \tag{6.68}$$

We observe that the leftover integrals of the above four equations, Eqs. (6.64)–(6.68) cancel.

Adding Eqs. (6.40)–(6.68) by parts, we arrive at the desired result.

VII. CONCLUSIONS

In this paper we have extended the S-matrix PT with *nonconserved* currents to the case of three boson vertices, with all three incoming momenta *off shell*. We have outlined in detail how the effective gauge-invariant three-boson vertices can be constructed, and we have given explicit closed expressions for the vertices γW^-W^+, ZW^-W^+, and χW^-W^+ in Eqs. (4.33), (4.34), and (4.35), respectively. The GI three-boson vertices were shown to satisfy naive tree-level Ward identities, which relate them to the GI gauge-boson self-energies previously constructed by the same method in [16]. The derivation of the aforementioned Ward identities relies on the sole requirement of complete gauge invariance of the S matrix element considered. In particular, no knowledge of the explicit closed form of the three-boson vertices involved is necessary, as long as they have been rendered individually ξ independent. The validity of one of these Ward identities has been proved explicitly, through a detailed diagrammatic one-loop analysis, in the context of three different gauges. The above proofs convincingly illustrate the gauge-invariant nature of the entire procedure. Most noticeably, the proof of the Ward identity in the unitary gauge supplies additional evidence that the PT endows the Green's functions computed in the unitary gauge with several desired theoretical properties, as already shown in [29] for the simpler case of the W self-energy.

Of particular interest is the further exploration of the recently advocated connection between the PT and BFM. Specifically, all cases studied thus far show that the PT Green's functions coincide with the BFM Green's functions, computed at $\xi_Q = 1$. Unfortunately, no general proof of this point exists yet. In Sec. VI C we presented a heuristic argument based on the structure of the Feynman rules in this particular gauge, which supports the general validity of this hypothesis, at least at the one-loop level. Because of the lack of a rigorous proof, however, additional individual cases may have to be examined. To that end one will have to construct physically relevant Green's functions via the PT and then compare them with the analogous Green's functions of the BFM at $\xi_Q = 1$. The general methodology presented in Sec. III and the closed explicit expressions reported in Sec. IV provide the starting point for such a detailed comparison. Furthermore, the general character of the Ward identities derived in this paper may provide additional clues towards a formal understanding of the PT algorithm. Results in this direction will be reported elsewhere.

Finally, we would like to point out that the Ward identities derived in Sec. V have already found application in the study of resonant amplitudes, most noticeably for the processes $\gamma e^- \to \mu^-\bar{\nu}_\mu\nu_e$ and $Ze^- \to \mu^-\bar{\nu}\mu\nu_e$, and they are crucial for the gauge-fixing parameter independence and U(1) electromagnetic gauge invariance of the final answer [35].

ACKNOWLEDGMENTS

One of us (K.P.) would like to thank V. Filippidis for technical support and K. Skenderis for discussions about the BFM. This work was supported in part by the National Science Foundation Grant No. PHY-9313781.

[1] J. M. Cornwall, in *Deeper Pathways in High Energy Physics*, edited by B. Kursunoglu, A. Perlmutter, and L. Scott (Plenum, New York, 1977), p. 683.
[2] J. M. Cornwall, Phys. Rev. D **26**, 1453 (1982).
[3] J. M. Cornwall, Phys. Rev. D **38**, 656 (1988).
[4] J. M. Cornwall, Physica A **158**, 97 (1989).
[5] J. M. Cornwall and J. Papavassiliou, Phys. Rev. D **40**, 3474 (1989).
[6] J. Papavassiliou, Phys. Rev. D **47**, 4728 (1993).
[7] J. M. Cornwall, R. Jackiw, and E. T. Tomboulis, Phys. Rev. D **10**, 2428 (1974); J. M. Cornwall and R. Norton, Ann. Phys. (N.Y.) **91**, 106 (1975).
[8] Even if one assumes that $\hat{d}$, $\hat{\Gamma}_3$, and $\hat{\Gamma}_4$, are individually GI, Ω still displays a residual dependence on the gauge-fixing parameter, stemming from the free part of the gluon propagators. Equation (1.1) is the necessary condition for the order-by-order cancellation of this residual gauge dependence.
[9] It is only after the gauge invariance of Ω has been guaranteed that one proceeds to obtain the SD equations for the GI Green's functions $\hat{d}$, $\hat{\Gamma}_3$, and $\hat{\Gamma}_4$ by means of a variational principle. To that end, one extremizes inde-

pendently the variations of $\Omega(\hat{d}, \hat{\Gamma}_3, \hat{\Gamma}_4)$ with respect to $\hat{d}$, $\hat{\Gamma}_3$, and $\hat{\Gamma}_4$, e.g., $\frac{\delta\Omega}{\delta\Delta} = 0$, $\frac{\delta\Omega}{\delta\Gamma_3} = 0$, and $\frac{\delta\Omega}{\delta\Gamma_4} = 0$, imposing Eq. (1.4) as an additional constraint.

[10] It is important to emphasize that the Ward identities of Eq. (1.4) make no reference to ghosts; they are valid, however, also in the context of covariant gauges after the application of the PT.

[11] R. Jackiw and K. Johnson, Phys. Rev. D **8**, 2386 (1973); J. M. Cornwall and R. Norton, *ibid.* **8**, 3338 (1973); E. Eichten and F. Feinberg, *ibid.* **10**, 2428 (1974).

[12] J. Papavassiliou, Phys. Rev. D **41**, 3179 (1990).

[13] G. Degrassi and A. Sirlin, Nucl. Phys. **B383**, 73 (1992); Phys. Rev. D **46**, 3104 (1992).

[14] G. Degrassi, B. Kniehl, and A. Sirlin, Phys. Rev. D **48**, R3963 (1993).

[15] J. Papavassiliou and C. Parrinello, Phys. Rev. D **50**, 3059 (1994).

[16] J. Papavassiliou, Phys. Rev. D **50**, 5958 (1994).

[17] K. Hagiwara, S. Matsumoto, and C. S. Kim, in *Proceedings of the 14th International Workshop "Weak Interactions and Neutrinos,"* edited by J. E. Kim and S. K. Kim (World Scientific, 1994), p. 19; K. Hagiwara, D. Haidt, C. S. Kim, and S. Matsumoto, Z. Phys. C **64**, 559 (1994).

[18] K. J. F. Gaemers and G. J. Gounaris, Z. Phys. C **1**, 259 (1979); K. Hagiwara, R. D. Peccei, D. Zeppenfeld, and K. Hikasa, Nucl. Phys. **B282**, 253 (1987).

[19] U. Baur and D. Zeppenfeld, Nucl. Phys. **B308**, 127 (1988); **B325**, 253 (1989); E. N. Argyres, F. K. Diakonos, O. Korakianitis, C. G. Papadopoulos, and W. J. Stirling, Phys. Lett. B **272**, 431 (1991); E. N. Argyres, G. Katsilieris, O. Korakianitis, C. G. Papadopoulos, K. Philippides, and W. J. Stirling, *ibid.* **280**, 324 (1992); F. K. Diakonos, O. Korakianitis, C. G. Papadopoulos, K. Philippides, and W. J. Stirling, *ibid.* **303**, 177 (1993).

[20] S. J. Brodsky and J. R. Hiller, Phys. Rev. D **46**, 2141 (1992); M. Clauson, E. Fahri, and R. L. Jaffe, *ibid.* **34**, 873 (1986); G. Belanger, F. Boudjema, and D. London, Phys. Rev. Lett. **65**, 2943 (1990); F. Boudjema, Phys. Rev. D **36**, 969 (1987); J. Wudka, in *Proceedings of the XXVIIIth Rencontre de Moriond "Electroweak Interactions and Unified Theories,"* Les Arcs, Savoie, France, 1993, edited by J. Tran Thanh Van (Editions Frontieres, Gif-sur-Yvette, France, 1993), pp. 441–448.

[21] K. Fujikawa, B. W. Lee, and A. I. Sanda, Phys. Rev. D **6**, 2923 (1972).

[22] E. N. Argyres, G. Katsilieris, A. B. Lahanas, C. G. Papadopoulos, and V. C. Spanos, Nucl. Phys. **B391**, 23 (1993).

[23] J. Papavassiliou and K. Philippides, Phys. Rev. D **48**, 4255 (1993).

[24] L. F. Abbott, Nucl. Phys. **B185**, 189 (1981) and references therein.

[25] A. Denner, S. Dittmaier, and G. Weiglein, Phys. Lett. B **333**, 420 (1994); S. Hashimoto, J. Kodaira, Y. Yasui, and K. Sasaki, Phys. Rev. D **50**, 7066 (1994); E. de Rafael and N. J. Watson (unpublished).

[26] Of course, one can apply the PT in the context of the BFM to eliminate the residual ξ_Q dependence when $\xi_Q \neq 1$. In that case one arrives again at precisely the same unique results as in any other gauge-fixing scheme [27].

[27] J. Papavassiliou, Phys. Rev. D **51**, 856 (1995).

[28] N. J. Watson, Phys. Lett. B **349**, 155 (1995).

[29] J. Papavassiliou and A. Sirlin, Phys. Rev. D **50**, 5951 (1994).

[30] K. Aoki, Z. Hioki, R. Kawabe, M. Konuma, and T. Muta, Prog. Theor. Phys. Suppl. **73**, 1 (1982).

[31] We emphasize again that, since the quantities constructed via the PT are ξ independent, any choice for the parameters ξ is legitimate.

[32] The diagrams where the pinching occurs at the fermion line on the left are exactly analogous to those where the pinching occurs at the fermion line on the right and are not shown.

[33] We remind the reader that the tadpole diagrams must also be included in the definition of the GI self-energies.

[34] (ii) and (iii) are one-particle-reducible graphs. The graphs in category (ii) become disconnected only after a gauge-boson line is cut. The graphs in (iii) become disconnected in an additional way, namely, by cutting the off-shell fermionic propagator.

[35] J. Papavassiliou and A. Pilaftsis, "A gauge independent approach to resonant transition amplitudes," Report No. hep-ph/9507246 (submitted to Phys. Rev. D).